Article

Cell Host & Microbe

Proton Motive Force Disruptors Block Bacterial Competence and Horizontal Gene Transfer

Graphical Abstract

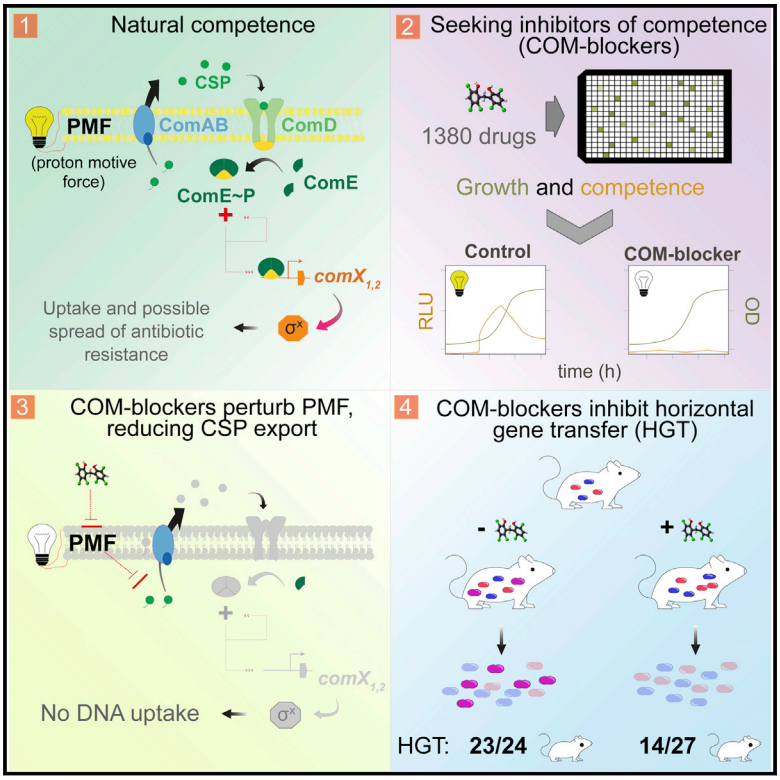

Highlights

- Competence development leads to DNA uptake and spread of antibiotic resistance
- Identification of competence inhibitors in *Streptococcus pneumoniae* (COM-blockers)
- COM-blockers act by disrupting the proton motive force, thereby reducing CSP export
- COM-blockers inhibit horizontal gene transfer in a murine model of infection

Authors

Arnau Domenech, Ana Rita Brochado, Vicky Sender, Karina Hentrich, Birgitta Henriques-Normark, Athanasios Typas, Jan-Willem Veening

Correspondence

jan-willem.veening@unil.ch

In Brief

Bacteria can take up exogenous DNA via competence. We identified compounds that prevent competence and horizontal gene transfer in *Streptococcus pneumoniae*. COM-blockers work by perturbing the proton motive force, thereby reducing the export of the quorum-sensing peptide that activates competence. COM-blockers could mitigate the spread of antibiotic resistance in pneumococcus.

Domenech et al., 2020, Cell Host & Microbe *27*, 1–12
April 8, 2020
https://doi.org/10.1016/j.chom.2020.02.002

CellPress

Please cite this article in press as: Domenech et al., Proton Motive Force Disruptors Block Bacterial Competence and Horizontal Gene Transfer, Cell Host & Microbe (2020), https://doi.org/10.1016/j.chom.2020.02.002

Cell Host & Microbe
Article

Proton Motive Force Disruptors Block Bacterial Competence and Horizontal Gene Transfer

Arnau Domenech,[1,2] Ana Rita Brochado,[3,6] Vicky Sender,[4] Karina Hentrich,[4] Birgitta Henriques-Normark,[4,5] Athanasios Typas,[3] and Jan-Willem Veening[1,2,7,8,*]
[1]Molecular Genetics Group, Groningen Biomolecular Sciences and Biotechnology Institute, Centre for Synthetic Biology, University of Groningen, Groningen 9747AG, the Netherlands
[2]Department of Fundamental Microbiology, Faculty of Biology and Medicine, University of Lausanne, Biophore Building, Lausanne 1015, Switzerland
[3]European Molecular Biology Laboratory, Genome Biology Unit, Heidelberg 69117, Germany
[4]Department of Microbiology, Tumor and Cell Biology, Karolinska Institutet, Stockholm 171 77, Sweden
[5]Department of Clinical Microbiology, Karolinska University Hospital Solna, Stockholm 171 76, Sweden
[6]Present address: Department of Microbiology, University of Würzburg, Biocenter, Am Hubland, Würzburg 97074, Germany
[7]Twitter: @JWVeening
[8]Lead Contact
*Correspondence: jan-willem.veening@unil.ch
https://doi.org/10.1016/j.chom.2020.02.002

SUMMARY

Streptococcus pneumoniae **is a commensal of the human nasopharynx that can also cause severe antibiotic-resistant infections. Antibiotics drive the spread of resistance by inducing *S. pneumoniae* competence, in which bacteria express the transformation machinery that facilitates uptake of exogenous DNA and horizontal gene transfer (HGT). We performed a high-throughput screen and identified potent inhibitors of *S. pneumoniae* competence, called COM-blockers. COM-blockers limit competence by inhibiting the proton motive force (PMF), thereby disrupting export of a quorum-sensing peptide that regulates the transformation machinery. Known chemical PMF disruptors and alterations in pH homeostasis similarly inhibit competence. COM-blockers limit transformation of clinical multi-drug-resistant strains and HGT in infected mice. At their active concentrations, COM-blockers do not affect growth, compromise antibiotic activity, or elicit detectable resistance. COM-blockers provide an experimental tool to inhibit competence and other PMF-involved processes and could help reduce the spread of virulence factors and antibiotic resistance in bacteria.**

INTRODUCTION

Even though *Streptococcus pneumoniae* (the pneumococcus) is part of the commensal microbiota of the human upper respiratory tract, it is also a major public health problem because it occasionally causes severe life-threatening infections, globally killing over a million people each year (Wahl et al., 2018). The alarming spread of penicillin- and multi-drug-resistant *S. pneumoniae* is a cause for concern, and despite the reduction in resistant infections after the introduction of several conjugate vaccines, non-vaccine serotype clones have rapidly emerged and spread (Kim et al., 2016). This phenomenon is especially accentuated among the at-risk population of people who undergo multiple courses of antimicrobial therapy per year (Domenech et al., 2014), which is often associated with treatment failure (Rzeszutek et al., 2004; Pletz et al., 2005; Zielnik-Jurkiewicz and Bielicka, 2015).

The rapid spread of antimicrobial resistance in *S. pneumoniae* can be largely attributed to transformation, which involves the uptake and assimilation of exogenous DNA. This leads to new genotypes and is an important mechanism of genome plasticity (Croucher et al., 2011; Chewapreecha et al., 2014; Gladstone et al., 2019). Transformation by horizontal gene transfer (HGT), the most common way DNA is acquired in *S. pneumoniae*, occurs mainly during colonization due to the simultaneous carriage of multiple pneumococcal strains (Donkor et al., 2011; Marks et al., 2012) or by the presence of closely related *Streptococci* such as *S. mitis*, which is considered one of the major reservoirs of antimicrobial resistance and virulence genes for *S. pneumoniae* (Janoir et al., 1999; Bryskier, 2002). In contrast with other competent bacteria such as *Haemophilus influenzae* or *Moraxella catarrhalis*, which are able to uptake DNA during their entire life cycle, *S. pneumoniae* needs to activate a physiological state called "competence" to express the transformation machinery required for the uptake and integration of the exogenous DNA (Claverys et al., 2009; Johnston et al., 2014) (Figure 1A). This is likely because pneumococci lack the canonical SOS-response and instead activate competence under stress conditions (Charpentier et al., 2012). Strikingly, several commonly used antimicrobials, such as fluoroquinolones, aminoglycosides, and amoxicillin-clavulanic acid, activate competence when present at sub-MIC levels (Prudhomme et al., 2006; Stevens et al., 2011; Slager et al., 2014; Domenech et al., 2018), and may thereby enhance the acquisition of virulence factors and antibiotic resistance alleles coming from the microbiota (Veening and Blokesch, 2017).

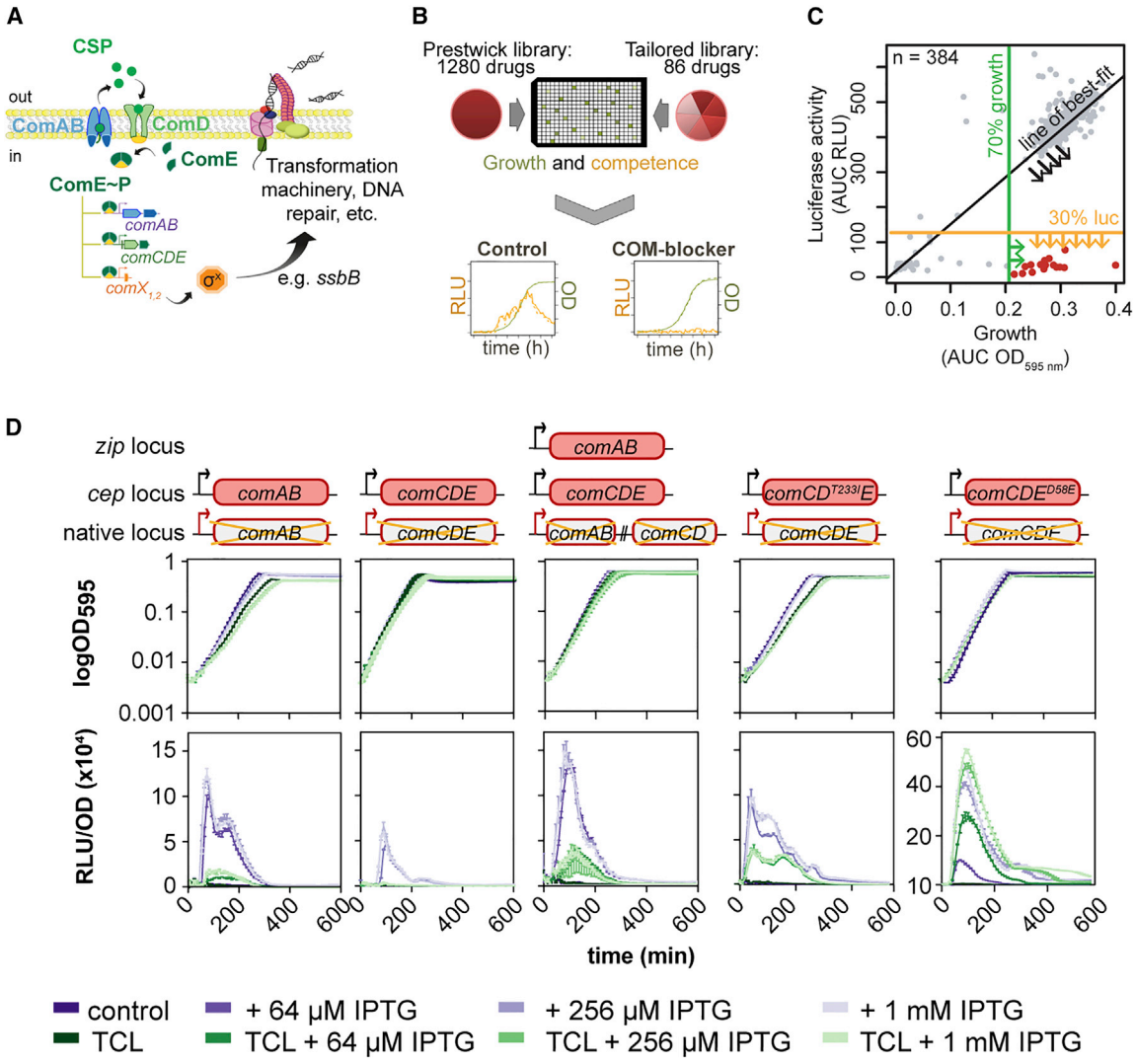

Figure 1. High-Throughput Screening to Identify COM-Blockers

(A) Overview of the regulatory network driving competence and transformation in *S. pneumoniae*. Two key operons are involved in competence activation, *comCDE* and *comAB*. The membrane transporter ComAB cleaves and exports the *comC*-encoded CSP, which then binds the membrane-bound histidine-kinase ComD, which autophosphorylates and transfers the phosphate group to the response regulator ComE. Phosphorylated ComE in turn activates the expression of the so-called "early" competence genes (Martin et al., 2000). One of them, *comX*, codes for a sigma factor (SigX), which is responsible for the activation of the so called "late" competence genes, including those required for transformation and DNA repair.

(B) Design of the COM-block screen. In control conditions (DMSO), the *S. pneumoniae* DLA3 strain (P_{ssbB}-*luc*) shows a normal growth rate (green line) and activation of competence, resulting in bioluminescence (orange). Specific COM-blockers do not affect the growth rate but prevent *ssbB* promoter activity. See also Tables S1 and S2.

(C) Example of COM-blocker identification from the high-throughput screen (data from Figure S1A). Scatterplots show the luminescence signal (area under the curve [AUC] of relative luminescence units [RLU]) versus growth (AUC: $OD_{595\ nm}$) obtained for each individual well per plate until 5 h of culture. The green, yellow, and black lines show the stringent criteria used to identify compounds that blocked natural competence development without drastically affecting growth, which were labeled COM-blockers, here shown in red. See also Table S3.

(D) Growth curves and detection of competence development was performed in C+Y medium at pH 7.5, permissive for natural competence. IPTG was added to the medium at the beginning at different final concentrations. Average of three replicates and standard error of the mean (SEM) are plotted. Strains used (left to right: ADP226, ADP107, ADP350, ADP272, and ADP148). Black arrows refer to the IPTG-inducible promoter P_{lac}, whereas red arrows indicate native promoters. See also Figure S2.

In an era in which antibiotic development has run dry, new strategies to preserve current drugs and minimize the impact of resistance are required. One proposed idea is to use drug combinations (Brochado et al., 2018; Tyers and Wright, 2019). For example, adjuvants with little or no antimicrobial activity on their own can be used to promote and/or complement the antibiotic activity in different ways such as inhibiting passive resistance or targeting host defense mechanisms (Wright, 2016). Other ideas involve searching for compounds that could reduce the evolution of resistance development (Ragheb et al., 2019;

Pribis et al., 2019) or the use of quorum-sensing analogues as modulators of pathogenic behaviors and players in biofilm formation (Zhu and Lau, 2011; Rutherford and Bassler, 2012; Yang et al., 2020).

Here, we describe inhibitors of competence that prevent transformation and the associated spread of resistant genes and virulence factors. We developed a high-throughput screen to identify these inhibitors, termed COM-blockers, and tested their activity *in vitro* and in an *in vivo* murine model of infection. We establish that the mechanism of action of COM-blockers is to disrupt the proton motive force (PMF). Pneumococcal competence is shown to be an exquisite probe to detect changes in the PMF given competence is inhibited at concentrations that do not affect cell growth. This class of small-molecule inhibitors provide insights into the molecular mechanisms underpinning pneumococcal competence development.

RESULTS

Identification of COM-Blockers

To identify small-molecule, FDA-approved agents with favorable pharmacokinetic and pharmacodynamic (PK/PD) characteristics that block pneumococcal competence, we screened a compound library of 1,280 drugs including antimicrobials (http://www.prestwickchemical.com) (Table S1). Given that the pneumococcal minimum inhibitory concentration (MIC) of most antibiotics in the library (~200) is below the tested concentration (20 μM), this setup inevitably prevents us from detecting the "competence-blocking ability" of most relevant antibiotics because of strong growth defects. To overcome this drawback, we additionally tested a self-assembled library of 86 compounds (tailored library; Table S2), mostly including clinically relevant antibiotics as well as biocides that were not represented in the initial library, and selected 6 pneumococcus-tailored drug concentrations over a range of 2-fold dilutions (Table S2). In total, we tested 1,366 compounds for their ability to inhibit competence development in *S. pneumoniae* (Figure 1B). As a reporter for natural competence (without addition of an exogenous competence-stimulating peptide [CSP]), we used the competence-specific induced *ssbB* promoter fused to firefly luciferase (strain DLA3, serotype 2; P_{ssbB}-*luc*) (Slager et al., 2014; Domenech et al., 2018). Luciferase activity and optical density were regularly measured along the growth to determine the individual effect of each drug on competence over 5 h. COM-blockers were identified as those compounds that strongly inhibited luciferase activity without a pronounced negative effect on growth (Figure S1A; STAR Methods). All experiments were done in duplicate and had high replicate correlation—average Pearson R > 0.95 (Figure S1B). In total, we identified 46 compounds (COM-blockers; Table S3) that inhibited competence at sub-inhibitory concentrations (below MIC_{90}).

To exclude the possibility that COM-blockers somehow interfere with luminescence detection, for instance, by reducing the amount of substrate entering the cell, we tested the effects of COM-blockers on a strain that constitutively expresses luciferase (Figure S1C). This showed that COM-blockers do not affect luciferase production and detection and instead specifically reduce P_{ssbB}-*luc* expression (Figure S1C). Two main groups of COM-blockers could be classified based on their known therapeutic activity and presumed mode of action: 20 compounds are known to affect membrane and/or ion homeostasis (Group 1), 10 are classified as antipsychotic drugs (Group 2), and the rest do not fall in these two groups (Group 3). We performed validation experiments (independent of the high-throughput screen) with 7 COM-blockers belonging to the three groups and confirmed strong competence inhibition (Figure S1D). From this initial screen, we describe results for the biocide triclosan (TCL) from Group 1, pimozide (PIM) from Group 2, and the antimalarial drug proguanil hydrochloride (PROG) from Group 3 as examples for further experiments, because they are well-studied compounds and showed very potent COM-blocking activities at low concentration.

Upregulation of Competence Cannot Bypass COM-Blocker Activity

To examine whether upregulation of the early operons *comAB* and/or *comCDE* could bypass the COM-blocking activity of TCL, PROG, and PIM, we constructed a suite of strains in which we could ectopically induce the competence genes by adding isopropyl β- d-1-thiogalactopyranoside (IPTG) (Figures 1D and S2). Upregulation of *comAB* resulted in rapid competence development; however, in the presence of COM-blockers, competence development was still nearly abolished. Inducing expression of the entire *comCDE* operon also led to competence activation but to a smaller extent compared to ComAB overproduction (Figures 1D and S2), likely because ComAB is rate-limiting in the development of competence (Martin et al., 2000). In all cases, COM-blockers counteracted the induction of *comAB* or *comCDE* and abolished competence. Similar effects were observed when both the *comAB* and the *comCDE* operons were induced simultaneously, indicating that these COM-blocking strategies are not easy to resolve and develop resistance by raising mutations that will upregulate different competence pathways.

COM-Blockers Perturb CSP Export

For a better understanding of how COM-blockers inhibit competence, we tested whether they alter any of the known membrane processes essential for competence development: the secretion of ComC (called CSP once outside the cell) by the ComAB exporter and/or the phosphorylation of ComE by ComD (Figure 1A). First, we evaluated whether the presence of TCL affected the interaction between ComD and ComE by adding exogenous CSP_1 at different times to the control strain (DLA3) and a *comAB* mutant (ADP342). Shortly after the addition of CSP_1, a rapid bioluminescence signal was detected in both strains; however, competence was switched off earlier in the *comAB* mutant, probably because this strain cannot amplify the competence signal by exporting extra CSP_1 in the common pool (Figure 2A). Furthermore, the addition of CSP_1 to cells treated with TCL also showed rapid competence activation similar to the control, indicating that ComD can recognize CSP and phosphorylate ComE in the presence of TCL. However, as observed for the *comAB* mutant, the wild-type DLA3 strain in the presence of TCL showed faster competence shut down, suggesting that TCL inhibits either CSP production or export (Figure 2A). In line with the observations that TCL decouples the CSP-ComD-ComE positive feedback (Figure 1A), the addition of TCL strongly reduced the activity of both P_{comAB} and

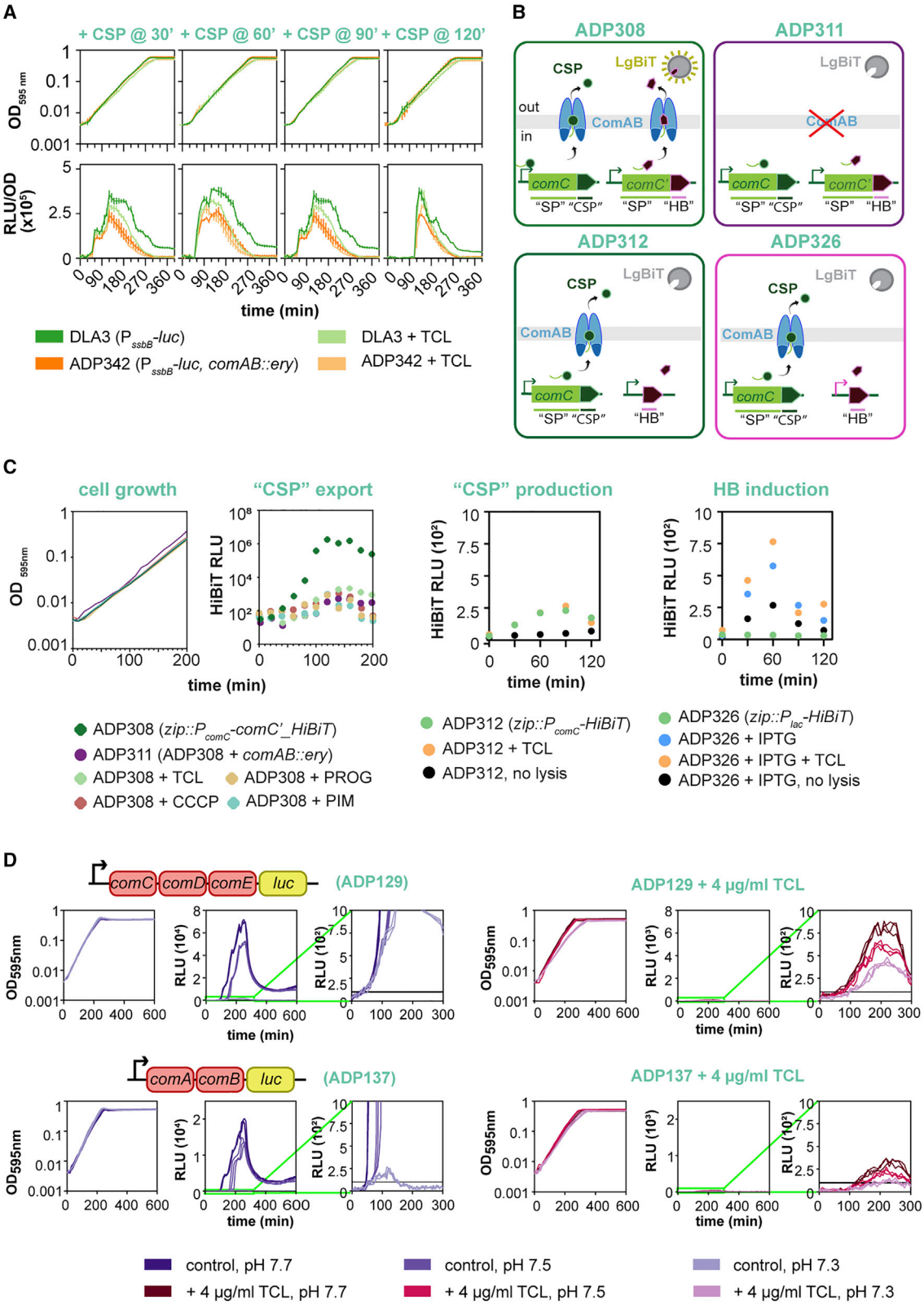

Figure 2. Triclosan Affects CSP Export

(A) Competence blocking by TCL is bypassed by addition of synthetic CSP_1. 100 ng/mL CSP_1 was added to the medium after 30 min, 60 min, 90 min, and 120 min to strains DLA3 (P_{ssbB}-*luc*) and ADP342 (P_{ssbB}-*luc*, *comAB::ery*). TCL was present at 4 µg/mL instead of 1 µg/mL to exacerbate the phenotype.

(legend continued on next page)

P_{comCDE} (Figure 2D). This potentially decreases the amount of CSP accumulated and thereby leads to a loss of competence development.

If this is the case, then the ectopic expression of a constitutively active mutant of ComD or ComE should be insensitive to COM-blockers. As the overproduction of ComD or ComE alone repressed competence because unphosphorylated ComE represses ComE-dependent promoters (Guiral et al., 2006), we constructed two strains in which the entire *comCDE* operon was under IPTG-inducible control, but whereby either the wild-type *comD* or *comE* genes were exchanged for two constitutively active mutants. The first mutant, $ComD^{T233I}$ (strain ADP272), constitutively phosphorylates ComE independent of the presence of CSP (Guiral et al., 2006), whereas the second, $ComE^{D58E}$ (strain ADP148), mimics the phosphorylated form of ComE, thus inducing competence even in the absence of CSP or ComD (Martin et al., 2013). $ComD^{T233I}$ showed a hypercompetent phenotype in presence of IPTG, though COM-blockers were still able to reduce competence activation to nearly half the luminescence production when $ComD^{T233I}$ was induced (Figures 1D and S2). The differences between the presence or absence of COM-blockers suggest that the competence feedback is still necessary to fully activate this strain, and the export of CSP boosts the positive feedback, increasing the bioluminescence signal, or that a fully intact PMF is required for ComD-ComE signaling. In contrast, competence was unaffected by COM-blockers when $ComE^{D58E}$ was induced (Figures 1D and S2).

Finally, to confirm whether CSP production and/or export are inhibited by COM-blockers, we employed a split-luciferase HiBiT-tag detection system to track the CSP export rate (Wang et al., 2018; Domenech et al., 2018). When HiBiT is expressed and exported out of the cell, it reacts with a HiBiT-dependent luciferase variant (LgBiT) added to the medium, resulting in bioluminescence (Figure 2B). First, the HiBiT tag was placed under the control of the *comCDE* promoter and coupled to the signal peptide sequence of *comC* (ADP308). When HiBiT is produced in this system, ComAB recognizes the leader signal, cleaves it and exports HiBiT. In the absence of ComAB (in strain ADP311), HiBiT is not matured and exported, so it accumulates in the cytoplasm and no luminescence is generated (Figure 2C, left). In the presence of COM-blockers, bioluminescence was abolished, indicating that HiBiT, and thereby CSP, were either not produced or were not exported. Finally, in the absence of the signal sequence (strain ADP312), HiBiT accumulated in the cytoplasm, and luminescence was not generated unless cells were lysed (Figure 2C).

COM-Blockers Disrupt the Proton Motive Force

To identify the molecular mechanism underlying the inhibition of competence, we analyzed the physiological effects of the COM-blockers on pneumococci. The results presented so far suggested that COM-blockers could inhibit competence due to an alteration of the PMF. Indeed, classical disrupters of the PMF (carbonylcyanide m-chlorophenylhydrazone [CCCP], nigericin, and valinomycin) were also highly effective in blocking competence (Figures 2C and S1D). We used specific fluorescent dyes to test the flux of H^+ and K^+ after addition of several COM-blockers to understand how they perturb the PMF (Figures 3A and 3B). TCL and PROG decrease the internal pH, but, in contrast to nigericin, both compounds also decrease intracellular potassium levels. Interestingly, PIM did not affect the internal pH but did affect K^+ uptake. This suggests that targeting the PMF is promising for blocking competence development, independent of the underlying mechanism of its disruption. To confirm that TCL decreases the intracellular pH, we tested the susceptibility of *S. pneumoniae* to TCL in a range of pH values. Indeed, the stepwise acidification of the medium by decreasing the pH resulted in increased susceptibility to TCL (Figure 3C).

To confirm whether pH homeostasis is essential for competence, we targeted the F_0F_1 proton ATPase complex, which is used to maintain pH homeostasis in *S. pneumoniae* (Clavé and Trombe, 1989). We used CRISPR interference (CRISPRi) (Liu et al., 2017) to reduce transcription of *atpE*, *atpA*, and *atpC,* three genes of the operon encoding the ATP synthase (Figure 4A). Indeed, the reduced expression of the *atp* genes (Figure 4B) led to a strong inhibition of competence. To confirm that the absence of bioluminescence was due to the block in competence and not to the absence of luciferase activity (given that this enzyme requires ATP to convert luciferine to oxyluciferine), we repeated the same experiments using a constitutive reporter. In this case, we did not observe significant differences (Figure 4C).

To strengthen the case for perturbations in the PMF causing COM-blocking effects, we searched for evidence of other COM-blockers that inhibit the F_0F_1 proton ATPase enzyme.

(B) Graphical representation of the HiBiT experiments. From left to right, top to bottom: (I) ComC (called CSP once outside the cell) and HiBiT are regulated by the *comCDE* promoter, and both precursors have a signal peptide sequence that is recognized, cleaved, and exported by ComAB (strain ADP308). Once outside the cell, HiBiT interacts with the soluble protein LgBiT and produces bioluminescence. (II) In the absence of ComAB (strain ADP311), HiBiT accumulates in the cytoplasm because it cannot be recognized and exported. (III and IV) HiBiT peptide expression is under control of P_{comCDE} promoter (ADP312) or under control of IPTG-inducible P_{lac} promoter (ADP326) without the leader sequence. In both cases, HiBiT is accumulated in the cytoplasm since it cannot be recognized and exported.

(C) CSP export is strongly reduced in presence of COM-blockers. Bioluminescence (RLU) can be correlated with CSP export. Left, CSP is exported until the saturation point (~10^7 RLU). The presence of COM-blockers abolished CSP export, showing similar background RLU to the *comAB* mutant strain (ADP311). To confirm that COM-blockers do not affect the expression of the HiBiT, ADP312 and ADP326 were grown in C+Y at pH 7.9 and samples were taken every 30 min for analysis and were lysed with 0.1% Triton X-100 and 2% deoxycholate. pH 7.9 used in this experiment allowed earlier competence development compared to the pH used in previous experiments (pH 7.5), thereby reducing the required amount of luciferine and number of reads to favor a rapid natural competence. Concentrations used: 4 μg/mL of TCL, CCCP, PROG, and PIM and 1 mM of IPTG. Only one replicate per condition is shown.

(D) Effects of triclosan (TCL) on the activity of the early competence promoters P_{comCDE} and P_{comAB}. Strains were grown in C+Y medium in permissive (pH 7.7 and 7.5) and non-permissive (pH 7.3) conditions for natural competence. In normal conditions, there is a basal expression of *comCDE* even at the low pH 7.3. However, the lower production at pH 7.3 results in smaller amounts of CSP accumulated and thereby less phosphorylated ComE (ComE~P) to amplify the competence positive feedback loop (Martin et al., 2013). TCL addition nearly completely blocks P_{comCDE} basal expression, which disrupts the positive feedback. Alike, in absence of ComE~P, basal expression of P_{comAB} is shut down in the lower pH and in presence of TCL. Three replicates per each condition are plotted.

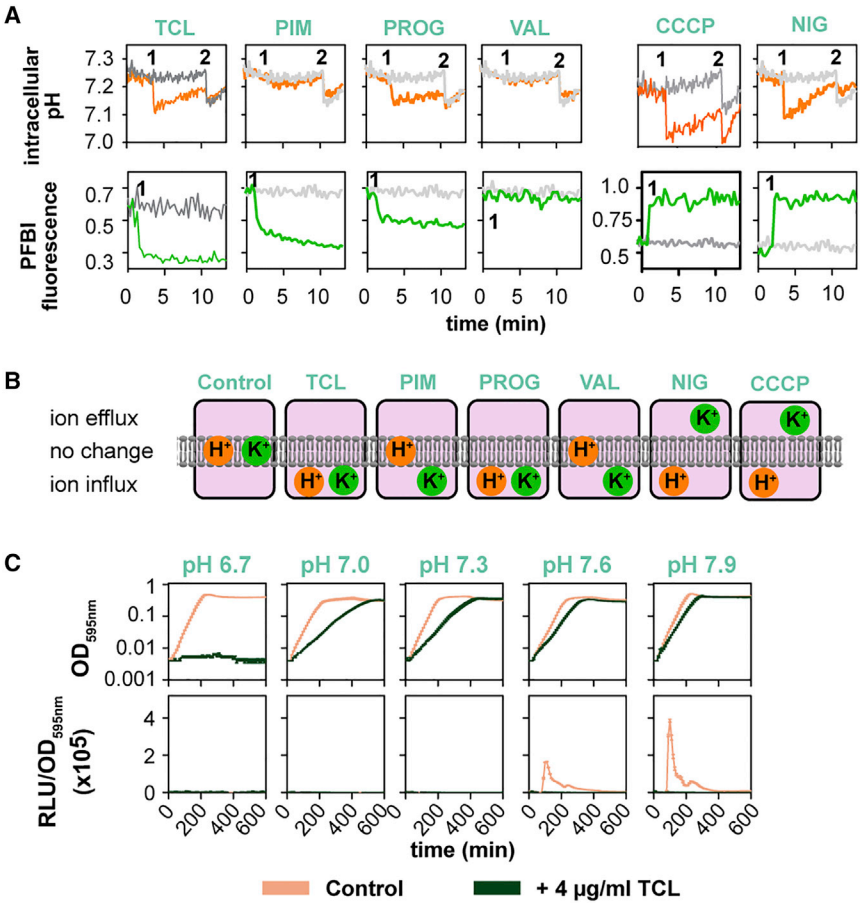

Figure 3. COM-Blockers Disrupt the Proton Motive Force

(A) Intracellular changes in pH (H^+) and potassium (K^+) after the addition of several COM-blockers: 4 μg/mL of TCL, PIM, and PROG or 0.5 μg/mL of nigericin (NIG) and valinomycin (VAL). NIG, an antiporter of H^+ and K^+, decreases the internal pH by exchanging H^+ and K^+ (Clementi et al., 2014). VAL makes selective pores for K^+ (Clementi et al., 2014). Upper panels: pneumococci were loaded with the pH-sensitive dye BCECF (50 μM). After the baseline was recorded, TCL (orange) or DMSO (gray) was added (1). In presence of TCL, PROG, and NIG, a drop in signal was observed, indicating a decrease in the internal pH. The addition of 20 μg/mL of NIG (2) collapses the PMF and equilibrates the external and internal pH. Lower panels: cells were incubated with PBFI/AM dye (5 μM) and treated (1) with COM-blockers (green) or DMSO (gray). Changes in fluorescence were recorded, showing that TCL, PIM, and PROG lead to increased intracellular accumulation of K^+. Contrary, NIG addition resulted in an extrusion of K^+ outside the cell.

(B) Summary of the effect on internal pH and potassium levels by the addition of several COM-blockers. TCL decreases the internal pH but also increases the cytoplasmic concentration of K^+.

(C) Effect of TCL on growth (upper) and competence activity (lower) of *S. pneumoniae* DLA3 grown in a range of pH values. Acidic medium increases the susceptibility of DLA3 to 4 μg/mL of TCL, with complete growth abolition at pH 6.7 and lower. Average of three replicates and SEM are plotted.

One well-known compound, optochin (ethylhydrocupreine hydrochloride), is an antibiotic classically used to differentiate *S. pneumoniae* (optochin-susceptible) from other α-hemolytic streptococci (optochin-resistant) (Muñoz et al., 1996; Martín-Galiano et al., 2001). However, pneumococcal optochin resistance has been reported by point mutations in *atpE*, a subunit of the F_0F_1 proton ATPase enzyme (Lund and Henrichsen, 1978). We first confirmed that optochin is a COM-blocker (Figure 4D) and then tested whether these two different amino acid changes in AtpE ($AtpE^{V48L}$ and $AtpE^{A49T}$) led to COM-blocker resistance. As expected, both mutations conferred resistance to optochin, which resulted in a loss of COM-blocking activity (Figure 4D). However, there was no loss of COM-blocking by TCL or PROG in AtpE mutants, because neither TCL nor PROG are expected to have direct interaction with the ATPase (Figures 4E and 4F). In total, we conclude that COM-blockers work by perturbing the PMF.

COM-Blockers Inhibit Competence in Clinical Multi-Drug-Resistant Strains

To test whether COM-blockers also work in other strains, we first examined an unencapsulated strain (ADP26), because the human nasopharynx is frequently colonized by non-typeable pneumococci characterized by a lack of capsule and higher HGT efficiencies (Sá-Leão et al., 2006). As shown in Figure 5A, competence was similarly inhibited in strain ADP26. Next, we tested several multi-drug-resistant pneumococcal strains belonging to worldwide Pneumococcal Molecular Epidemiology Network (PMEN) lineages (McGee et al., 2001) with similar results (Figure 5A). Finally, we analyzed the effects of COM-blockers in two closely related *Streptococci* belonging to the mitis group: *S. mitis* and *S. sanguinis*, which are abundant in the human microbiome and considered reservoirs of antibiotic-resistance genes and virulence factors (Janoir et al., 1999; Bryskier, 2002). Both *S. mitis* and *S. sanguinis* demonstrated similar competence inhibition profiles compared to pneumococcal strains (Figure 5A).

COM-Blockers Prevent Transformation and HGT Transfer

Though the expression of *ssbB* is a good indicator of competence (Prudhomme et al., 2006; Slager et al., 2014; Domenech et al., 2018), we wanted to examine if COM-blockers such as TCL indeed inhibit the downstream process of transformability. We first tested whether TCL would efficiently prevent transformation when naked DNA carrying relatively short homology regions (approximately 1 kb) was provided directly to the growth medium (Table S4). Second, we tested the transfer of a replicative plasmid, and finally, we co-cultured two different pneumococcal strains (with a different antibiotic-resistant determinant inserted at different chromosomal positions) allowing competence-dependent HGT to take place via the uptake of

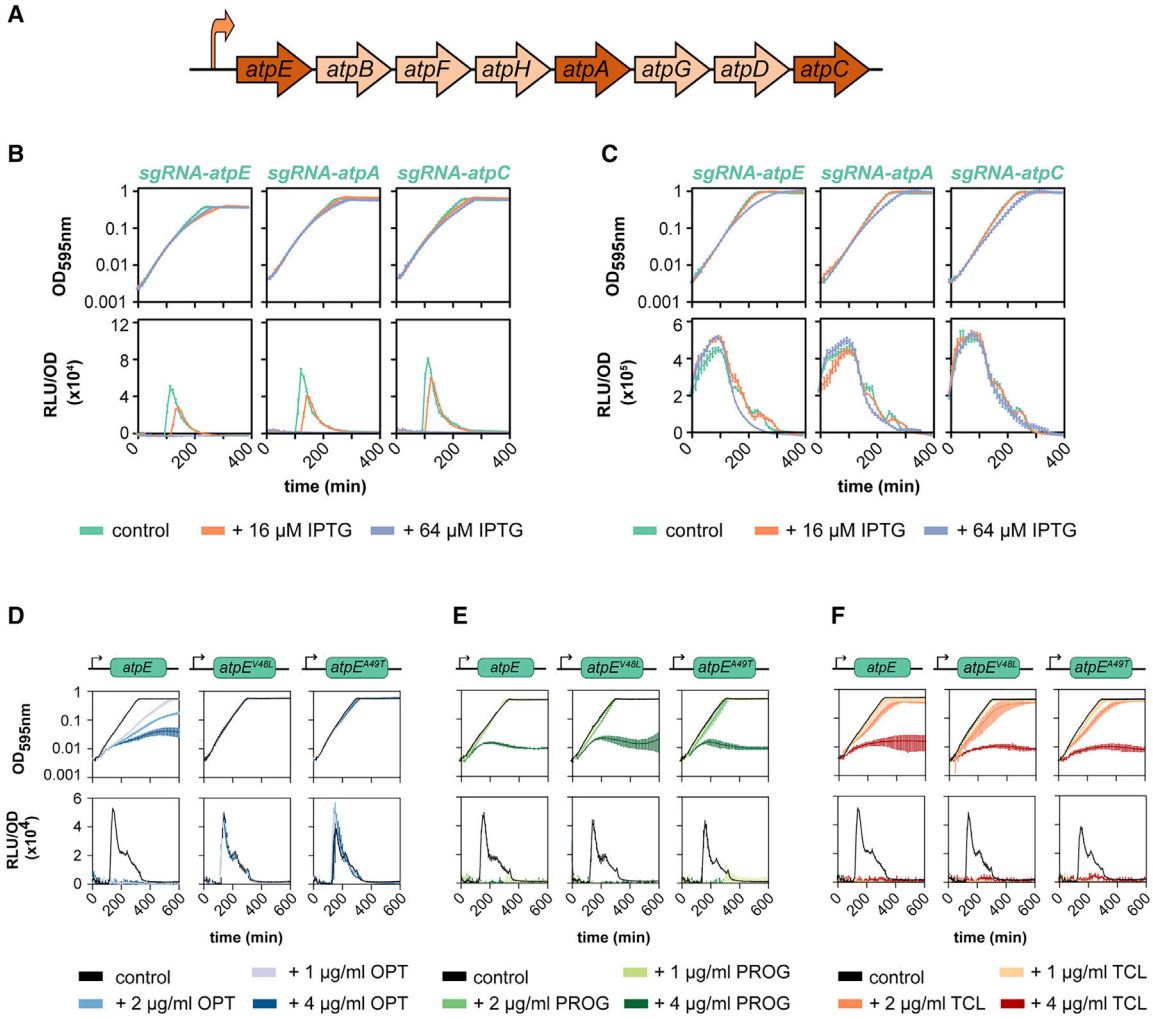

Figure 4. F_0F_1 ATPase Is Essential for Natural Competence Induction

(A) Schematic overview of the operon encoding ATP synthase. Dark color indicates the genes targeted in (B) and (C).

(B) Depletion (by CRISPRi) of gene products related to ATP synthase results in an inhibition of competence (no bioluminescence activity in presence of increasing concentration of IPTG). Average of three replicates and SEM are plotted.

(C) Depletion of these gene products does not affect the luciferase activity in strains constitutively expressing this enzyme. Average of three replicates and SEM are plotted.

(D) Effect of two mutations in AtpE subunit of ATPase of *S. pneumoniae* on optochin (OPT) activity. Left, growth curves and competence induction of *S. pneumoniae* DLA3 strain without (black) or with a range of optochin. The presence of the compound affects growth rates and competence development. Center and right, the presence of any of both mutations in AtpE (strains ADP279 and ADP280, respectively) restores the growth rates and natural competence development. Average of three replicates and SEM are plotted.

(E and F) Effect of the same mutations on PROG (E) and TCL (F). Both $AtpE^{V48L}$ (strain ADP279) and $AtpE^{A49T}$ (strain ADP280) substitutions have no effect on growth rates or competence inhibition for either PROG or TCL. Average of three replicates and SEM are plotted.

See also Figure S3 and Tables S7 and S8.

chromosomal DNA (Table S5). A drastic inhibition of transformation was detected in the presence of TCL in all three experiments (Tables S4 and S5). In addition, HGT was also evaluated in presence of the COM-blockers PIM and PROG, with identical results (Table S5). The total number of cells recovered was similar under all the conditions, showing that the addition of COM-blockers at competence-blocking concentrations did not affect cell viability. These results were reproduced in the presence of ciprofloxacin and kanamycin, two antibiotics that promote competence (Table S5) (Slager et al., 2014).

Importantly, TCL also potently prevented the acquisition of exogenous DNA in clinical strains expressing different capsular types (Figure 5B). All clinical strains showed an MIC_{90} for growth of 16 μg/mL TCL, with exception of *S. mitis* (32 μg/mL TCL). We then tested the minimal transformation inhibition concentration ($MTIC_{90}$), defined as the lowest concentration to inhibit the uptake of exogenous DNA in 90% of the population. Overall, 1 μg/mL of TCL (3.13%–6.25% of the MIC_{90}) was enough to reach $MTIC_{90}$ in several clinical strains (Figure 5B). Interestingly, TCL blocked HGT in clinical strains expressing two different

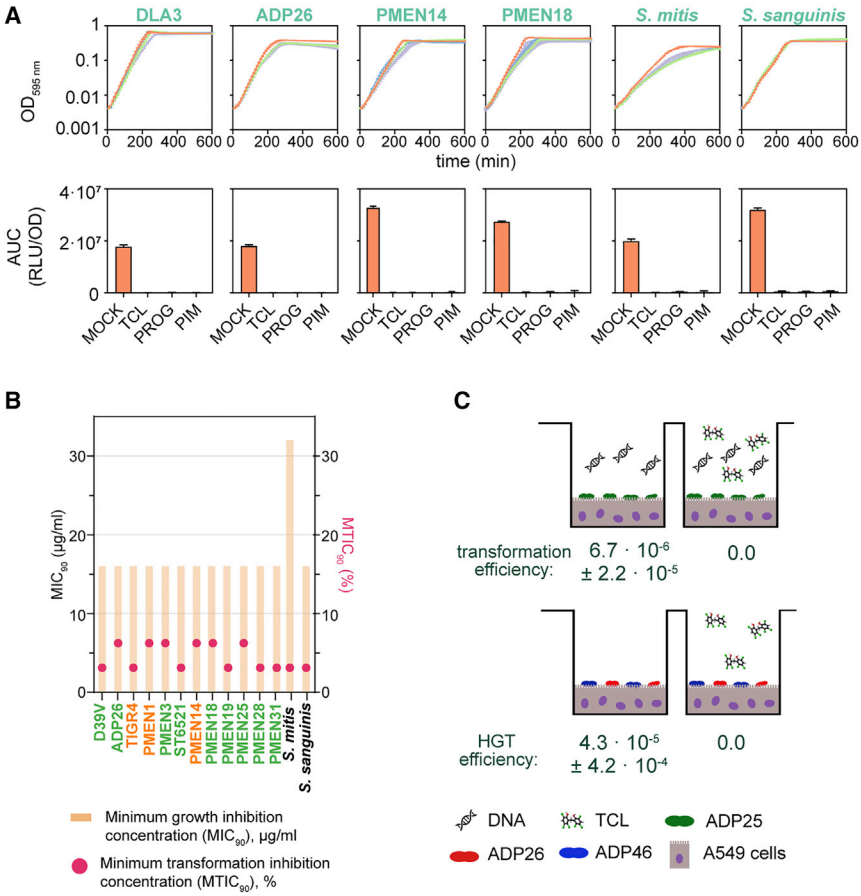

Figure 5. COM-Blockers Work in Clinical Strains and Prevent HGT in an Epithelial Colonization Model

(A) Growth curves and competence activity (AUC of RLU) of *S. pneumoniae* variants (P_{ssbB}-*luc*) of D39V (DLA3) and its unencapsulated variant (*cps::cat*, ADP26); two clinical strains, PMEN14 (ADP49) and PMEN18 (ADP50); and two *Streptococci* of the mitis Group, *S. mitis* (ADP51) and *S. sanguinis* (ADP53), in presence of COM-blockers. Strains were grown in C+Y medium in permissive conditions for natural competence development (pH 7.5). All strains showed bioluminescence activity in absence of COM-blocker (orange), and the addition of COM-blocker abolished competence development at concentrations of 1 μg/mL. An average of three replicates and the SEM are plotted.

(B) Percentage of the TCL MIC_{90} required for inhibition of transformation ($MTIC_{90}$) in several clinical strains and two closely related *Streptococci*. Green labeled strains express pherotype CSP-1, whereas orange labeled strains express pherotype CSP-2.

(C) Upper, unencapsulated D39V bacteria (strain ADP25, green) adhered to a monolayer of A549 human lung epithelial cells previously fixed (purple) were able to take up naked DNA under permissive conditions (pH 7.5). However, the addition of TCL at 2 μg/mL completely blocked transformation. Lower, HGT efficiency between two identical unencapsulated strains adhered to a monolayer of A549 human cells. ADP26 and ADP46 differ only in the presence of a resistance marker integrated in different regions of the genome (tetracycline and kanamycin, respectively). The presence of 2 μg/mL of TCL completely blocked HGT between both strains.

See also Tables S4 and S5.

CSP types, CSP_1 and CSP_2 (green and orange, respectively; Figure 5B).

To test whether TCL also inhibits competence development under conditions more closely resembling human colonization, we performed experiments in a human lung epithelial cell colonization model. For these experiments, planktonic bacteria were washed to ensure that transformation and HGT occur only in bacteria colonizing the surface of the human A549 cells. To increase natural transformation and HGT efficiency, we used unencapsulated pneumococci (ADP25, ADP26, and ADP46), because the absence of the capsule enhances adhesion thereby increasing HGT (Hammerschmidt et al., 2005). As shown in Figure 5C and Tables S4 and S5, transformation and HGT were also blocked by TCL in this adherence model.

PROG Treatment Reduces *In Vivo* HGT in a Mouse-Infection Model

To test whether COM-blockers would be able to reduce HGT *in vivo*, we setup an HGT mouse model (Figure 6A). We chose PROG as the COM-blocker because it has been used safely in humans for over a decade as an antimalarial drug. C57BL/6 mice were infected intraperitoneally with a 1:1 mixture of two genetically identical strains except for their antibiotic resistance marker (strains DLA3 and MK134, 10^7 bacteria each). Then, 15 min post infection, mice were either mock treated or treated with 6 mg/kg PROG and bacterial load, and HGT was assessed 12 h post infection by plating on selective plates (Figure 6A). PROG treatment at the concentration used did not affect the total number of colony-forming units (CFUs) (Table S6). For all but one mock-treated animal (n = 23 out of 24), a high number of transformants were detected demonstrating that pneumococcus efficiently performs HGT during infection in mice (Figure 6B; Table S6). Importantly, PROG treatment significantly reduced HGT efficiency, and in 14 out of 27 animals no transformants were detected at all ($p = 0.0087$).

Undetectable Resistance toward COM-Block Activity

We next set out to confirm whether TCL could be used for prolonged periods of time without losing its COM-blocking activity. Wild-type strain D39V was continuously exposed to increasing concentrations of TCL. After 30 days of consecutively plating eight independent lineages in three concentrations of TCL (10 μg/mL, 15 μg/mL, and 20 μg/mL), the maximum concentration that we detected growth at was 15 μg/mL of TCL, though the cells were not able to grow during continuous exposure at this concentration (Figure S3A). Importantly, 1 μg/mL of TCL could still block competence in all lineages throughout the 30 days (Figure S3B), indicating that loss of COM-blocking activity is also undetectable even after prolonged exposures.

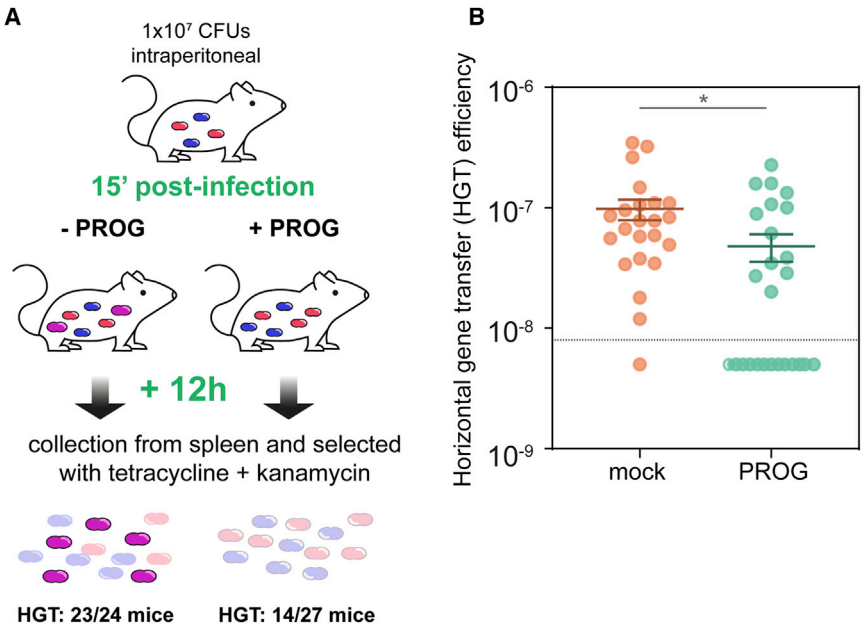

Figure 6. Reduced *In Vivo* HGT by PROG during Pneumococcal Infection

(A) Schematic representation of the *in vivo* HGT infection model. Genetically identical strains DLA3 (tetracycline resistant, red diplococci) and MK134 (kanamycin resistant, blue diplococci) were used in a 1:1 ratio (10^7 bacteria of each strain) to infect C57BL/6 mice intraperitoneally. After 12 h, bacteria from the spleens were plated on agar media containing kanamycin (CFU's of strain DLA3), tetracycline (CFU's of strain MK134), no antibiotics (all bacteria), or tetracycline and kanamycin (HGT events, purple diplococci).

(B) The intraperitoneal injection of PROG (6 mg/kg body weight) 15 min after infection significantly inhibited HGT between both strains in the spleen. Horizontal line indicates limit of transformants detection (no colonies on the transformation plates). At least 25 mice per condition were tested. *Statistically significant reduced HGT in presence of PROG, t test analysis, $p < 0.05$.

See also Table S6.

A recent study showed that *E. coli* and *S. aureus* can develop tolerance to certain clinical antibiotics when they are previously exposed to MIC concentrations of TCL (Westfall et al., 2019). Despite the fact that our COM-blockers act at sub-MIC concentrations, we tested whether *S. pneumoniae* continuously exposed to TCL (lineages 1, 2, and a mix of all 8 lineages from Figure S3A) developed reduced susceptibility to clinically relevant antibiotics. As shown in Table S7, the MICs to the tested antibiotics were constant over time, showing that TCL does not promote cross-resistance toward antibiotics in *S. pneumoniae*. Finally, we also did not detect rapid resistance development against COM-blockers TCL, PROG, and PIM in a standard fluctuation assay, whereas rifampicin resistant mutants were readily selected for in this assay (Table S8).

DISCUSSION

Antibiotic-resistant infections remain a major cause of concern, because of their continued increased global incidence and the lack of new antibiotics. In addition, several antibiotics used for the treatment of *S. pneumoniae* are able to promote competence development and thereby the uptake of exogenous DNA (Prudhomme et al., 2006; Stevens et al., 2011; Slager et al., 2014; Domenech et al., 2018). Hence, new strategies to preserve current drugs and minimize the impact of resistance are required.

Here, we screened for small FDA-approved molecules that could inhibit antibiotic-induced competence induction (COM-blockers). Most of these compounds are currently used for the treatment of other human diseases and proven to have good PK/PD characteristics. Our initial high-throughput screening of 1,366 compounds included a total of 79 antibiotics currently used for therapeutic treatments, however, none of them were able to inhibit the natural competence development by their own. Nevertheless, 46 compounds belonging to several ATC (anatomical therapeutic chemical) classification systems showed a potent activity blocking competence without affecting bacterial growth. Most of the compounds have a putative effect on the membrane stability and/or ion homeostasis. To further study their underlying mode of action, we selected a biocide (TCL), an antimalarial drug (PROG), and an antipsychotic (PIM), because they are well-studied with a very potent COM-blocking activity at low concentration (16 to 32 times lower than the MIC; Figure S1D).

Using several approaches, we confirmed that COM-blockers are potent inhibitors of competence, transformation, and HGT in planktonic growth but also in a model of colonization in A549 human cell line and in an *in vivo* model of murine infection (Figures 5 and 6; Tables S4 and S5). These results were also reproduced using clinical pneumococcal strains expressing different capsular types and a different CSP type (Figure 5B), suggesting that COM-blockers act by blocking a common pathway and would block DNA uptake in any pneumococcal strain, no matter the CSP allele.

We found that COM-blockers disrupt the PMF affecting selective ion flux, with different underlying mechanisms (Figure 3). This suggests that targeting the PMF is promising for blocking competence development, independent of the way to disrupt it. The bacterial cell membrane has become an appealing target because it is essential and has a highly conservative structure (Dias and Rauter, 2019). Indeed, at a concentration 10 times higher than required to abolish competence, COM-blockers also affect pneumococcal growth (Figure 4). However, the toxicity of drugs interfering with the bacterial membrane at MIC concentrations is a cause of concern, because human cells can be compromised as well (Dias and Rauter, 2019).

We demonstrated that PMF disruption by COM-blockers affects CSP export. Consequently, ComD will not autophosphorylate and will not phosphorylate ComE, thereby also reducing P_{comAB} and P_{comCDE} transcription (Figure 7). Given that the competence pathway is tightly regulated at different levels to prevent spontaneous activation when it is not required, a minimal disruption of CSP export is enough to unbalance the

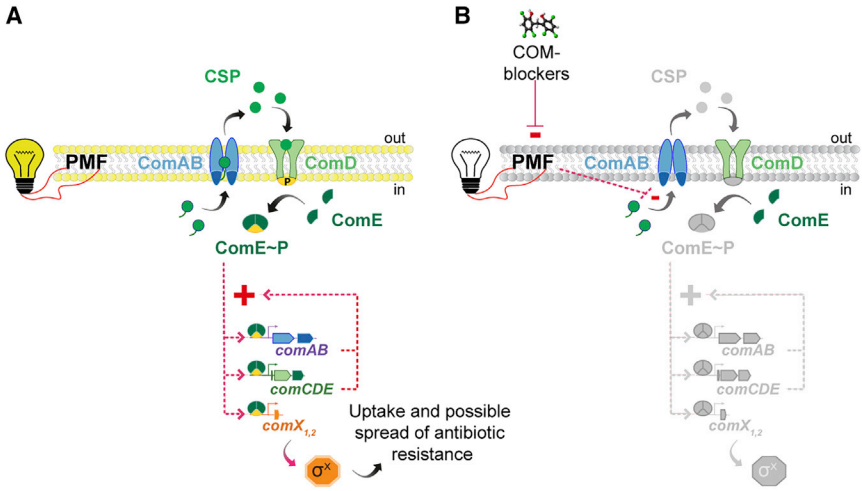

Figure 7. Model of COM-Blocker Activity

(A) The PMF maintains membrane homeostasis and thus, membrane-associated processes such as ComAB activity. ComAB cleaves and exports the *comC*-encoded CSP. CSP then stimulates the phosphorylation of ComE via ComD (see Figure 1A for more details), creating a positive feedback loop, amplifying the signal (by increasing *comAB* and *comCDE* expression) and inducing the expression of *comX*, which encodes for the sigma factor SigX, responsible for the activation of the transformation machinery, which can lead to the acquisition of antibiotic resistance.

(B) COM-blockers disrupt the PMF, thereby preventing ComAB from exporting enough CSP to trigger the positive feedback (gray pathway). The absence of feedback results in a decreased expression of both *comAB* and *comCDE* operons, the absence of competence, and the expression of the transformation machinery.

accumulation of ComE and prevent competence development (Figure 7). For this reason, the COM-blockers mentioned here disrupt competence without attenuating cell growth, because they already work at sub-inhibitory concentrations (16%–32% below the MIC). The identification of COM-blockers and their mode of action—perturbing the PMF, thereby reducing CSP export—has now provided an explanation for a long-standing question in the field as to why competence is so sensitive to external pH (Moreno-Gámez et al., 2017). Under acidic conditions, ATP synthase has to work hard to pump out protons and maintain membrane homeostasis. Given ComAB, and probably many other exporters, is sensitive to cellular ATP levels and/or membrane homeostasis, reduced intracellular ATP levels or perturbed membrane homeostasis will immediately lead to reduced ComC cleavage and export as CSP (Figure 7). This then, in turn, will not lead to activation of ComE and the positive feedback loop that normally results in even higher production of CSP (Figure 7). Hence, the competence pathway is shown to be an exquisite probe to detect changes in the PMF, well before growth defects appear.

Given that COM-blockers act at sub-inhibitory concentrations, we expect a low selection pressure for resistance compared to drugs affecting cell viability like antibiotics. We performed two different approaches to promote the acquisition of resistance: long-term exposure to increasing concentrations of TCL (Figure S3) and a standard fluctuation assay (Table S8). The lack of resistance development or antibiotic tolerance observed in both experiments might be due to TCL having multiple targets and pneumococcus lacking the main TCL target, the enoyl-acyl carrier protein (ACP) reductase FabI, present in other bacteria such as *E. coli* or *Staphylococcus aureus* (pneumococcus has an isozyme of FabI named FabK, which does not interact with TCL) (Heath and Rock, 2000). The fluctuation assay also confirmed the lack of resistance to PROG and PIM, in contrast to the antibiotic rifampicin, for which a rapid selection of mutants was observed after 24 h (Table S8). In addition, we also demonstrated that eventual mutations that could lead to the overexpression of the early competence operons (Figures 1D and S2) cannot bypass COM-blocking activity. Altogether our results suggest that the activity of COM-blockers such as TCL, PROG, and PIM cannot be easily compromised by the acquisition of point mutations or changes on the metabolism such as changes in the competence pathway or possible overexpression of pumps, as observed for *E. coli* (McMurry et al., 1998).

PMF plays a crucial role in several biological processes such as coupling membrane-associated enzymes, transport of solutes across the membrane, or cytoplasmic pH maintenance. The COM-blockers described here represent an experimental tool to study this process because they act at sub-inhibitory concentrations before compromising cell growth. We demonstrated that COM-blockers can be used in an *in vivo* model, and, unlike the classical CCCP PMF disruptor, COM-blockers are already FDA approved and some of them, such as PROG, have been used safely as an antimalarial medication since its approval in 2000 (https://www.accessdata.fda.gov). Future studies will be needed to test whether "anti-evolution" drugs, such as the here-described COM-blockers, can be realistically used in combination with antibiotics to prevent the spread of antibiotic resistance and virulence factors in pathogens.

STAR★METHODS

Detailed methods are provided in the online version of this paper and include the following:

- KEY RESOURCES TABLE
- LEAD CONTACT AND MATERIALS AVAILABILITY
- EXPERIMENTAL MODEL AND SUBJECT DETAILS
  - Bacterial Strains and Growth Conditions
  - Human Cell Line and Growth Conditions
  - Mice and Spleen Collection
- METHOD DETAILS
  - Competence Assays
  - High Throughput Screen of Competence Inhibitors
  - *In Vitro* HGT between *S. pneumoniae* Strains
  - Transformation Assays
  - HGT Assays in Bacteria Adhered to Human Airway Cells
  - *In Vivo* HGT Assay

SUPPLEMENTAL INFORMATION

Supplemental Information can be found online at https://doi.org/10.1016/j.chom.2020.02.002.

A video abstract is available at https://doi.org/10.1016/j.chom.2020.02.002#mmc4.

ACKNOWLEDGMENTS

We are grateful to Mark van der Linden and Peter Hermans for providing the collection of clinical PMEN strains tested in this study. We thank Marco Oggioni for insightful discussions regarding the pneumococcal F_0F_1 ATPase and are grateful to all members of the Veening lab for stimulating discussions. This work was supported by the Swiss National Science Foundation (project grant 31003A_172861 to J.-W.V.) and a JPIAMR grant (50-52900-98-202 to J.-W.V. and A.T.) from the Netherlands Organization for Health Research and Development (ZonMW). This work was also supported by the Swedish Research Council, the Knut and Alice Wallenberg Foundation, and the Swedish Foundation for Strategic Research (to B.H.-N.) A.D. was supported by Marie Skłodowska-Curie fellowship 657546.

AUTHOR CONTRIBUTIONS

Conceptualization, A.D. and J.-W.V.; Methodology: A.D., V.S., A.R.B., and K.H.; Writing – Original Draft, A.D. and J.-W.V.; Writing – Review & Editing: A.D., V.S., A.R.B, K.H., A.T., B.H.-N., and J.-W.V.

DECLARATION OF INTERESTS

A.D. and J.-W.V. author the International Patent Application No. PCT/NL2017/050671 WO/2018/070874. Authors declare no other competing interests.

Received: December 10, 2019
Revised: January 14, 2020
Accepted: February 3, 2020
Published: March 3, 2020

REFERENCES

Brochado, A.R., Telzerow, A., Bobonis, J., Banzhaf, M., Mateus, A., Selkrig, J., Huth, E., Bassler, S., Zamarreño Beas, J., Zietek, M., et al. (2018). Species-specific activity of antibacterial drug combinations. Nature *559*, 259–263.

Bryskier, A. (2002). Viridans group streptococci: a reservoir of resistant bacteria in oral cavities. Clin. Microbiol. Infect. *8*, 65–69.

Charpentier, X., Polard, P., and Claverys, J.P. (2012). Induction of competence for genetic transformation by antibiotics: convergent evolution of stress responses in distant bacterial species lacking SOS? Curr. Opin. Microbiol. *15*, 570–576.

Chewapreecha, C., Harris, S.R., Croucher, N.J., Turner, C., Marttinen, P., Cheng, L., Pessia, A., Aanensen, D.M., Mather, A.E., Page, A.J., et al. (2014). Dense genomic sampling identifies highways of pneumococcal recombination. Nat. Genet. *46*, 305–309.

Clavé, C., and Trombe, M.C. (1989). DNA uptake in competent *Streptococcus pneumoniae* requires ATP and is regulated by cytoplasmic pH. FEMS Microbiol. Lett. *53*, 113–118.

Claverys, J.P., Martin, B., and Polard, P. (2009). The genetic transformation machinery: composition, localization, and mechanism. FEMS Microbiol. Rev. *33*, 643–656.

Clementi, E.A., Marks, L.R., Roche-Håkansson, H., and Håkansson, A.P. (2014). Monitoring changes in membrane polarity, membrane integrity, and intracellular ion concentrations in Streptococcus pneumoniae using fluorescent dyes. J. Vis. Exp. *84*, e51008.

CLSI (Clinical and Laboratory Standards Institute) (2018). Performance Standards for Antimicrobial Susceptibility Testing, 28th Edition (Clinical and Laboratory Standards Institute).

Croucher, N.J., Harris, S.R., Fraser, C., Quail, M.A., Burton, J., van der Linden, M., McGee, L., von Gottberg, A., Song, J.H., Ko, K.S., et al. (2011). Rapid pneumococcal evolution in response to clinical interventions. Science *331*, 430–434.

Dias, C., and Rauter, A.P. (2019). Membrane-targeting antibiotics: recent developments outside the peptide space. Future Med. Chem. *3*, 211–228.

Domenech, A., Ardanuy, C., Tercero, A., García-Somoza, D., Santos, S., and Liñares, J. (2014). Dynamics of the pneumococcal population causing acute exacerbations in COPD patients in a Barcelona hospital (2009-12): comparison with 2001-04 and 2005-08 periods. J. Antimicrob. Chemother. *69*, 932–939.

Domenech, A., Slager, J., and Veening, J.W. (2018). Antibiotic-Induced Cell Chaining Triggers Pneumococcal Competence by Reshaping Quorum Sensing to Autocrine-Like Signaling. Cell Rep. *25*, 2390–2400.e3.

Donkor, E.S., Bishop, C.J., Gould, K., Hinds, J., Antonio, M., Wren, B., and Hanage, W.P. (2011). High levels of recombination among *Streptococcus pneumoniae* isolates from the Gambia. MBio *2*, e00040–11.

Gladstone, R.A., Lo, S.W., Lees, J.A., Croucher, N.J., van Tonder, A.J., Corander, J., Page, A.J., Marttinen, P., Bentley, L.J., Ochoa, T.J., et al.; Global Pneumococcal Sequencing Consortium (2019). International genomic definition of pneumococcal lineages, to contextualise disease, antibiotic resistance and vaccine impact. EBioMedicine *43*, 338–346.

Guiral, S., Hénard, V., Granadel, C., Martin, B., and Claverys, J.P. (2006). Inhibition of competence development in *Streptococcus pneumoniae* by increased basal-level expression of the ComDE two-component regulatory system. Microbiology *152*, 323–331.

Hammerschmidt, S., Wolff, S., Hocke, A., Rosseau, S., Müller, E., and Rohde, M. (2005). Illustration of pneumococcal polysaccharide capsule during adherence and invasion of epithelial cells. Infect. Immun. *73*, 4653–4667.

Heath, R.J., and Rock, C.O. (2000). A triclosan-resistant bacterial enzyme. Nature *406*, 145–146.

Janoir, C., Podglajen, I., Kitzis, M.D., Poyart, C., and Gutmann, L. (1999). *In vitro* exchange of fluoroquinolone resistance determinants between *Streptococcus pneumoniae* and viridans *streptococci* and genomic organization of the *parE-parC* region in *S. mitis*. J. Infect. Dis. *180*, 555–558.

Johnston, C., Martin, B., Fichant, G., Polard, P., and Claverys, J.P. (2014). Bacterial transformation: distribution, shared mechanisms and divergent control. Nat. Rev. Microbiol. *12*, 181–196.

Kim, L., McGee, L., Tomczyk, S., and Beall, B. (2016). Biological and Epidemiological Features of Antibiotic-Resistant *Streptococcus pneumoniae* in Pre- and Post-Conjugate Vaccine Eras: a United States Perspective. Clin. Microbiol. Rev. *29*, 525–552.

Liu, X., Gallay, C., Kjos, M., Domenech, A., Slager, J., van Kessel, S.P., Knoops, K., Sorg, R.A., Zhang, J.R., and Veening, J.W. (2017). High-throughput CRISPRi phenotyping identifies new essential genes in *Streptococcus pneumoniae*. Mol. Syst. Biol. *13*, 931.

Lund, E., and Henrichsen, J. (1978). Laboratory Diagnosis, Serology and Epidemiology of *Streptococcus pneumoniae*. In Methods in Microbiology, *Vol. 12*, T. Bergan and J.R. Norris, eds. (Academic Press), pp. 241–262.

Marks, L.R., Reddinger, R.M., and Hakansson, A.P. (2012). High levels of genetic recombination during nasopharyngeal carriage and biofilm formation in *Streptococcus pneumoniae*. MBio *3*, e00200–e00212.

Martin, B., Prudhomme, M., Alloing, G., Granadel, C., and Claverys, J.P. (2000). Cross-regulation of competence pheromone production and export in the early control of transformation in *Streptococcus pneumoniae*. Mol. Microbiol. *38*, 867–878.

Martin, B., Soulet, A.L., Mirouze, N., Prudhomme, M., Mortier-Barrière, I., Granadel, C., Noirot-Gros, M.F., Noirot, P., Polard, P., and Claverys, J.P.

(2013). ComE/ComE~P interplay dictates activation or extinction status of pneumococcal X-state (competence). Mol. Microbiol. *87*, 394–411.

Martín-Galiano, A.J., Ferrándiz, M.J., and de la Campa, A.G. (2001). The promoter of the operon encoding the F_0F_1 ATPase of *Streptococcus pneumoniae* is inducible by pH. Mol. Microbiol. *41*, 1327–1338.

McGee, L., McDougal, L., Zhou, J., Spratt, B.G., Tenover, F.C., George, R., Hakenbeck, R., Hryniewicz, W., Lefévre, J.C., Tomasz, A., and Klugman, K.P. (2001). Nomenclature of major antimicrobial-resistant clones of *Streptococcus pneumoniae* defined by the pneumococcal molecular epidemiology network. J. Clin. Microbiol. *39*, 2565–2571.

McMurry, L.M., Oethinger, M., and Levy, S.B. (1998). Overexpression of *marA, soxS*, or *acrAB* produces resistance to triclosan in laboratory and clinical strains of *Escherichia coli*. FEMS Microbiol. Lett. *166*, 305–309.

Moreno-Gámez, S., Sorg, R.A., Domenech, A., Kjos, M., Weissing, F.J., van Doorn, G.S., and Veening, J.W. (2017). Quorum sensing integrates environmental cues, cell density and cell history to control bacterial competence. Nat. Commun. *8*, 854.

Muñoz, R., García, E., and De la Campa, A.G. (1996). Quinine specifically inhibits the proteolipid subunit of the F_0F_1 H^+ -ATPase of *Streptococcus pneumoniae*. J. Bacteriol. *178*, 2455–2458.

Pletz, M.W.R., McGee, L., Burkhardt, O., Lode, H., and Klugman, K.P. (2005). Ciprofloxacin treatment failure in a patient with resistant *Streptococcus pneumoniae* infection following prior ciprofloxacin therapy. Eur. J. Clin. Microbiol. Infect. Dis. *24*, 58–60.

Pribis, J.P., García-Villada, L., Zhai, Y., Lewin-Epstein, O., Wang, A.Z., Liu, J., Xia, J., Mei, Q., Fitzgerald, D.M., Bos, J., et al. (2019). Gamblers: An Antibiotic-Induced Evolvable Cell Subpopulation Differentiated by Reactive-Oxygen-Induced General Stress Response. Mol. Cell *74*, 785–800.e7.

Prudhomme, M., Attaiech, L., Sanchez, G., Martin, B., and Claverys, J.P. (2006). Antibiotic stress induces genetic transformability in the human pathogen *Streptococcus pneumoniae*. Science *313*, 89–92.

Ragheb, M.N., Thomason, M.K., Hsu, C., Nugent, P., Gage, J., Samadpour, A.N., Kariisa, A., Merrikh, C.N., Miller, S.I., Sherman, D.R., and Merrikh, H. (2019). Inhibiting the Evolution of Antibiotic Resistance. Mol. Cell *73*, 157–165.e5.

Rutherford, S.T., and Bassler, B.L. (2012). Bacterial quorum sensing: its role in virulence and possibilities for its control. Cold Spring Harb. Perspect. Med. *2*, a012427.

Rzeszutek, M., Wierzbowski, A., Hoban, D.J., Conly, J., Bishai, W., and Zhanel, G.G. (2004). A review of clinical failures associated with macrolide-resistant *Streptococcus pneumoniae*. Int. J. Antimicrob. Agents *24*, 95–104.

Sá-Leão, R., Simões, A.S., Nunes, S., Sousa, N.G., Frazão, N., and de Lencastre, H. (2006). Identification, prevalence and population structure of non-typable *Streptococcus pneumoniae* in carriage samples isolated from preschoolers attending day-care centres. Microbiology *152*, 367–376.

Slager, J., Kjos, M., Attaiech, L., and Veening, J.W. (2014). Antibiotic-induced replication stress triggers bacterial competence by increasing gene dosage near the origin. Cell *157*, 395–406.

Stevens, K.E., Chang, D., Zwack, E.E., and Sebert, M.E. (2011). Competence in *Streptococcus pneumoniae* is regulated by the rate of ribosomal decoding errors. MBio *2*, e00071–11.

Tyers, M., and Wright, G.D. (2019). Drug combinations: a strategy to extend the life of antibiotics in the 21st century. Nat. Rev. Microbiol. *17*, 141–155.

Veening, J.W., and Blokesch, M. (2017). Interbacterial predation as a strategy for DNA acquisition in naturally competent bacteria. Nat. Rev. Microbiol. *15*, 629.

Wahl, B., O'Brien, K.L., Greenbaum, A., Majumder, A., Liu, L., Chu, Y., Lukšić, I., Nair, H., McAllister, D.A., Campbell, H., et al. (2018). Burden of *Streptococcus pneumoniae* and *Haemophilus influenzae* type b disease in children in the era of conjugate vaccines: global, regional, and national estimates for 2000-15. Lancet Glob. Health *6*, e744–e757.

Wang, C.Y., Patel, N., Wholey, W.Y., and Dawid, S. (2018). ABC transporter content diversity in *Streptococcus pneumoniae* impacts competence regulation and bacteriocin production. Proc. Natl. Acad. Sci. USA *115*, E5776–E5785.

Westfall, C., Flores-Mireles, A.L., Robinson, J.I., Lynch, A.J.L., Hultgren, S., Henderson, J.P., and Levin, P.A. (2019). The Widely Used Antimicrobial Triclosan Induces High Levels of Antibiotic Tolerance *In Vitro* and Reduces Antibiotic Efficacy up to 100-Fold *In Vivo*. Antimicrob. Agents Chemother. *63*, e02312–e02318.

Wright, G.D. (2016). Antibiotic Adjuvants: Rescuing Antibiotics from Resistance. Trends Microbiol. *24*, 862–871.

Yang, Y., Lin, J., Harrington, A., Cornilescu, G., Lau, G.W., and Tal-Gan, Y. (2020). Designing cyclic competence-stimulating peptide (CSP) analogs with pan-group quorum-sensing inhibition activity in *Streptococcus pneumoniae*. Proc. Natl. Acad. Sci. USA *117*, 1689–1699.

Yuzenkova, Y., Gamba, P., Herber, M., Attaiech, L., Shafeeq, S., Kuipers, O.P., Klumpp, S., Zenkin, N., and Veening, J.W. (2014). Control of transcription elongation by GreA determines rate of gene expression in *Streptococcus pneumoniae*. Nucleic Acids Res. *42*, 10987–10999.

Zhu, L., and Lau, G.W. (2011). Inhibition of competence development, horizontal gene transfer and virulence in *Streptococcus pneumoniae* by a modified competence stimulating peptide. PLoS Pathog. *7*, e1002241.

Zielnik-Jurkiewicz, B., and Bielicka, A. (2015). Antibiotic resistance of *Streptococcus pneumoniae* in children with acute otitis media treatment failure. Int. J. Pediatr. Otorhinolaryngol. *79*, 2129–2133.

STAR★METHODS

KEY RESOURCES TABLE

REAGENT or RESOURCE	SOURCE	IDENTIFIER
Bacterial and Virus Strains		
Bacterial strains are listed in Table S9	This paper	N/A
Chemicals, Peptides, and Recombinant Proteins		
Nano-Glo® HiBiT Extracellular Detection System	Promega	N2420
D-Luciferine	Synchem	CAS: 115144-35-9
Triclosan	Sigma	CAS: 3380-34-5
Proguanil hydrochloride	Sigma	CAS: 637-32-1
Pimozide	Sigma	CAS: 2062-78-4
BCECF, AM	Thermofisher	B1150
PBFI	Thermofisher	P1265MP
Prestwick library	N/A	www.prestwickchemical.com
Critical Commercial Assays		
Vybrant® MTT Cell proliferation assay kit	ThermoFisher	V13154
Experimental Models: Cell Lines		
Human: A549 epithelial cells	ATCC	CCL-185
Experimental Models: Organisms		
Six to eight-week-old male C57BL/6 mice	Charles River Laboratories	N/A
Software and Algorithms		
Code for HTS analysis	This paper	https://github.com/veeninglab/Domenech_et.al_2020

LEAD CONTACT AND MATERIALS AVAILABILITY

Further information and requests for resources and reagents should be directed to and will be fulfilled by the Lead Contact, Jan-Willem Veening (jan-willem.veening@unil.ch).

This study did not generate new unique reagents.

EXPERIMENTAL MODEL AND SUBJECT DETAILS

Bacterial Strains and Growth Conditions

Bacterial strains used in this study are listed in Table S9. Growth conditions of bacterial cells were described previously (Slager et al., 2014). Briefly, *S. pneumoniae* was grown in C+Y medium (pH 6.8, non-permissive conditions for natural competence induction), at 37°C and stored at −80°C in C+Y with 14.5% glycerol at $OD_{595\ nm}$ of 0.4. Determination of minimum inhibitory concentration (MIC) and minimum bactericidal concentration (MBC), was performed following the Clinical Laboratory Standards Institute (CLSI) methods (CLSI, 2018).

Human Cell Line and Growth Conditions

The cell line A549 (human lung carcinoma cell line) was used for *in vitro* experiments as follows: cells were seeded in 96-well plates at a density of $1.5 \cdot 10^6$ cells/cm^2 and maintained in GlutaMAX media (GIBCO®) at 37°C + 5% CO_2.

Mice and Spleen Collection

All experiments were performed in accordance with the local ethical committee (Stockholms Norra djurfösöksetiska nämnd). Six- to eight-week-old male C57BL/6 mice (Charles River Laboratories) were infected intraperitoneally with a 1:1 mixture of 1×10^7 CFU of two *S. pneumoniae* strains. For some experiments, mice were treated intraperitoneally with 6 mg/kg Proguanil hydrochloride (dissolved in sterile PBS/DMSO; 1.2%) or were mock-treated at 15 min post infection. At 12 h after infection, the mice were sacrificed, and spleens were collected. All mice were housed under specific pathogen-free conditions at Karolinska Institutet, Division of Comparative Medicine.

METHOD DETAILS

Competence Assays

The *S. pneumoniae* strains were cultured in a Tecan Infinite F200 PRO allowing for real-time monitoring of competence induction *in vitro*. *S. pneumoniae* was grown to OD_{595} 0.4 in C+Y pH 6.8 ± 0.05 (non-permissive conditions for natural competence induction) at 37°C. This pre-culture was diluted 100-fold in C+Y pH 7.5 ± 0.05 (permissive conditions for natural competence induction) containing 0.45 mg/mL of luciferine and then incubated in 384 or 96-wells microtiter plates with no shaking. Growth ($OD_{595\ nm}$) and luciferase activity (RLU) were measured every 10 min during 14 h, with at least three replicates per condition, except for high-throughput screening where we did duplicates. Expression of the *luc* gene (only if competence is activated) results in the production of luciferase and thereby in the emission of light (Slager et al., 2014). An average of 3 replicates and the standard error of the mean (SEM) are shown unless indicated.

High Throughput Screen of Competence Inhibitors

The Prestwick library was tested against the DLA3 (P_{ssbB}-*luc*) strain, in order to identify potential competence inhibitors. This library consists of 1280 FDA- and EMA-approved compounds (arranged in 4x384-wells microtiter plates), including a broad variety of antimicrobials and other drugs covering a wide range of chemical structures and therapeutic effects (http://www.prestwickchemical.com). Competence and growth assays were done simultaneously, in duplicate, in 384-wells microtiter plates containing 100 μl as described above, with a unique concentration of 20 μM for all compounds. The self-assembled pneumococcus tailored library containing 86 relevant clinical antimicrobials and several biocides in a range of 6 serial dilutions was tested using an identical setup. The library was assembled in 1x384-wells microtiter plate, with 4 concentrations per drug, over a 2-fold serial dilution. Starting concentrations of all individual compounds are listed on Table S1. This library was tested twice – once at the concentrations described in Table S1, and a second time with 1/4 of those. This enabled us to expand the concentration range per drug from 4 to 6 concentrations, along 2-fold serial dilutions. We obtained duplicates for both cases, full and 1/4 initial drug concentration. All liquid handling involving drugs and bacterial cultures was done with a Biomek FX liquid handler (Beckman Coulter). Plates were sealed with breathable membranes (Breathe-Easy®).

Here we define competence-blocking compounds – COM-blockers – as all compounds that inhibit competence as measured by luciferase activity under control of the *ssbB* promoter, and do not strongly halt growth. We used Area Under the Curve (AUC) until 5 h culture-time to describe growth ($OD_{595\ nm}$) and luciferase activity/competence (RLU) per well. Data reproducibility was assessed by Pearson correlation between the 2 replicates of each library plate (4 plates Prestwick library & 2 plates tailored library). We obtained very high reproducibility across replicates: 0.95 for growth and 0.94 for luciferase activity on average across all plates (Figure S1B). The vast majority of tested compounds do not show any specific effect on luciferase activity when compared to growth – when growth is decreased, luciferase activity will also decrease accordingly (Figure S1A). COM-blockers will deviate from this rule, as they will block the luciferase activity, while minimally affecting bacterial growth. High confidence COM-blockers satisfy the following stringent criteria (Figure S1A): a) below 7.5% quantile of the residuals of the line of best-fit luciferase activity versus growth; b) luciferase activity is below 70% of the median luciferase activity across all compounds in the plate and c) growth is at least 70% of median growth across all compounds in the plate. Relaxing these cutoffs causes lower agreement between the 2 replicates. Data analysis was done per individual plate, in order to account for eventual batch-effects that could occur across the different plates.

In Vitro HGT between *S. pneumoniae* Strains

We used the DLA3 (tetracycline resistant) and MK134 (kanamycin resistant) strains, which are naturally competent and are genetically identical, with exception of the locus where P_{ssbB}-*luc* was inserted, and the antimicrobial marker used (Table S4). Strains were grown to $OD_{595\ nm}$ 0.4 in C+Y pH 6.8 at 37°C (non-permissive conditions for natural competence activation). Then, both strains were mixed 1:1 in C+Y pH 6.8 to avoid spontaneous competence induction, and a mixed 100-fold dilution of both strains were grown in C+Y pH 7.5 (permissive conditions) to $OD_{595\ nm}$ to promote the transfer of genes. Afterward, serial dilution of cultures were plated without antibiotics (for the recovery of the total viable counts) and with the combination of 250 μg/mL of kanamycin plus 1 μg/mL tetracycline. The experiments were performed adding either 1 μg/mL or 2 μg/mL of TCL, and comparing with the control condition without TCL. Each experimental condition was independently performed at least three times. Individual precultures and the initial 1:1 mixture were also plated to confirm the absence of recombinants prior to the experiment. A total of 10 recombinant colonies were picked and both tetracycline- and kanamycin-resistant genes were amplified and Sanger sequenced to confirm the HGT.

For the replicative plasmid experiments, we used strain PGs6 (erythromycin-resistant) as donor (Yuzenkova et al., 2014), and strain ADP65 (kanamycin- and gentamycin-resistant) as recipient. The experiments were performed as indicated above, but plating in Columbia blood agar containing all three antibiotics (0.25μg/mL of erythromycin, 250 μg/mL of kanamycin and 20μg/mL of gentamycin). Plates were supplemented with the three antibiotics in order to nearly exclude the possibility of HGT from the recipient to the donor strain.

Transformation Assays

The wild-type D39V *S. pneumoniae* strain was grown to OD_{595} 0.4 in C+Y pH 6.8 at 37°C. This pre-culture was diluted 100-fold in C+Y pH 7.5 (permissive conditions) and 1 μg/mL or 2 μg/mL of TCL was added to the culture. After 150 min of incubation at 37°C (time required for natural competence induction, data not shown), 1 μg/mL of plasmid pLA18 (carrying the tetracycline-resistance determinant *tetM* (Slager et al., 2014), was added (Table S9 for plasmid information). The cultures were incubated at 37°C for 1 h30min and

then serial dilutions were plated either with or without 1 μg/mL of tetracycline. Transformation efficiency was calculated by dividing the number of transformants by the total number of viable count. Three independent replicates of each condition was performed.

HGT Assays in Bacteria Adhered to Human Airway Cells

The same experiments previously described were reproduced in *S. pneumoniae* adhered to a monolayer of human airway cells. A549 cells were incubated in 96-well plates in a density of $1.5e^6$ cells/cm^2, and grown at 37°C with 5% CO_2. After incubation, cells were washed twice with PBS and were fixed in 4% paraformaldehyde for 10 min. Then they were washed three times with PBS and were inoculated with a *S. pneumoniae* preculture in C+Y at OD 0.04. After 10 min, the 96 well plate was spun down 1 min at 2000 g. and the supernatant was removed. Wells were washed with PBS in order to remove planktonic cells, and fresh media supplemented with TCL and/or antibiotics were added in order to reproduce the experiments described above.

In Vivo HGT Assay

Six- to eight-week-old male C57BL/6 mice (Charles River Laboratories) were infected intraperitoneally with a 1:1 mixture of 1×10^7 CFU of DLA3 (tetracycline resistant) and 1×10^7 CFU of MK134 kanamycin resistant). The individual strains were kept separately on ice, mixed and immediately inoculated into animals to prevent the induction of competence prior to injection. For some experiments, mice were treated intraperitoneally with 6 mg/kg Proguanil hydrochloride (dissolved in sterile PBS/DMSO; 1.2%) or were mock-treated at 15 min post infection. At 12 h after infection, the mice were sacrificed, and spleen was collected. Enumeration of bacterial load was performed by plating serial dilutions on blood agar to estimate total CFU/mouse. Individual precultures and the initial 1:1 mixture were also plated to confirm the absence of recombinants. For enumeration of transformants the same samples were also plated on blood agar with 1 μg/mL tetracycline and 200 μg/mL kanamycin. Transformation efficiency was calculated by dividing the number of transformants by the total number of viable counts. Transformation occurred after the mice were challenged, as we did not detect any transformants in the bacterial mixture used to infect the animals. Significant outliers were excluded after applying the Grubb's test ($P < 0.005$).

Nano-Glo HiBiT Extracellular Detection System

Cells were pre-cultured in C+Y (pH 6.8) at 37°C to an $OD_{595\ nm}$ of 0.1, washed and diluted as explained before in C+Y (pH 7.9). Experiments were started with an inoculation density of OD_{595nm} 0.001. Every 20 min, 5 μl of the Nano-Glo® Extracellular Detection System reagent was added as specified in the manufacturer's instructions, and bioluminescence was detected in 96-wells plates with a Tecan Infinite 200 PRO luminometer at 37°C. Additionally, media and PBS samples were used as controls. Bioluminescence was measured right after the reagent addition. Two replicates for each time point and condition were tested.

Monitoring of Ions Fluxes

Cultured *S. pneumoniae* ADP25 cells at $OD_{595\ nm}$ 0.4 were washed and resuspended in buffer (5 mM HEPES buffer, 20 mM glucose, 100 mM KCl, pH 7.4). The measurement of the intracellular fluxes of K^+ and H^+ were analyzed using the appropriate dyes: PFBI, AM; and BCECF, AM; respectively, and following the protocol detailed on the reference (Clementi et al., 2014). Valinomycin, Nigericin and CCCP were used as controls of proton-motive force disturbers.

Measuring Mutation Rates Using the Fluctuation Assay

S. pneumoniae D39V was grown to OD_{595} 0.4 in C+Y pH 6.8 ± 0.05 at 37°C. Then, on the basis that $OD_{595\ nm}$ 0.1 contains $1.5x10^8$ colony forming units per ml (CFU/mL) (Moreno-Gámez et al., 2017), $6x10^8$ CFU's were plated onto Colombia blood agar, containing MIC or 2X MIC concentrations of the COM-blockers TCL, PROG and PIM (16 μg/mL and 32 μg/mL for each compound). Extra plates containing rifampicin (0.03 μg/mL and 0.06 μg/mL) were used as positive control for the rapid selection of mutants. Three independent biological replicates were performed.

Number of colonies were counted after 24 h and 48 h, and re-streaked with the same concentration of antibiotic (Table S8). Then *rpoB* of ten spontaneously resistant colonies from rifampicin treatment was analyzed by Sanger sequencing with the primer CGGTGACTCCTGCAGATATCCTTGCTGAG to exclude false positive colonies.

QUANTIFICATION AND STATISTICAL ANALYSIS

Data analysis was performed using GraphPad Prism, Microsoft Excel, R version 2.15.1 and RStudio Version 1.0.136.

Data shown in plots are represented as mean of at least three replicates ± SEM, as stated in the figure legends. Exact number of replicates for each experiment are enclosed in their respective figure legends. t test analysis ($p < 0.05$) was used to compare differences on the transformation and HGT experiments.

DATA AND CODE AVAILABILITY

The code generated during this study for the HTS analysis, together with the raw files are available at https://github.com/veeninglab/Domenech_et.al_2020.

Cell Host & Microbe, Volume *27*

Supplemental Information

Proton Motive Force Disruptors Block Bacterial Competence and Horizontal Gene Transfer

Arnau Domenech, Ana Rita Brochado, Vicky Sender, Karina Hentrich, Birgitta Henriques-Normark, Athanasios Typas, and Jan-Willem Veening

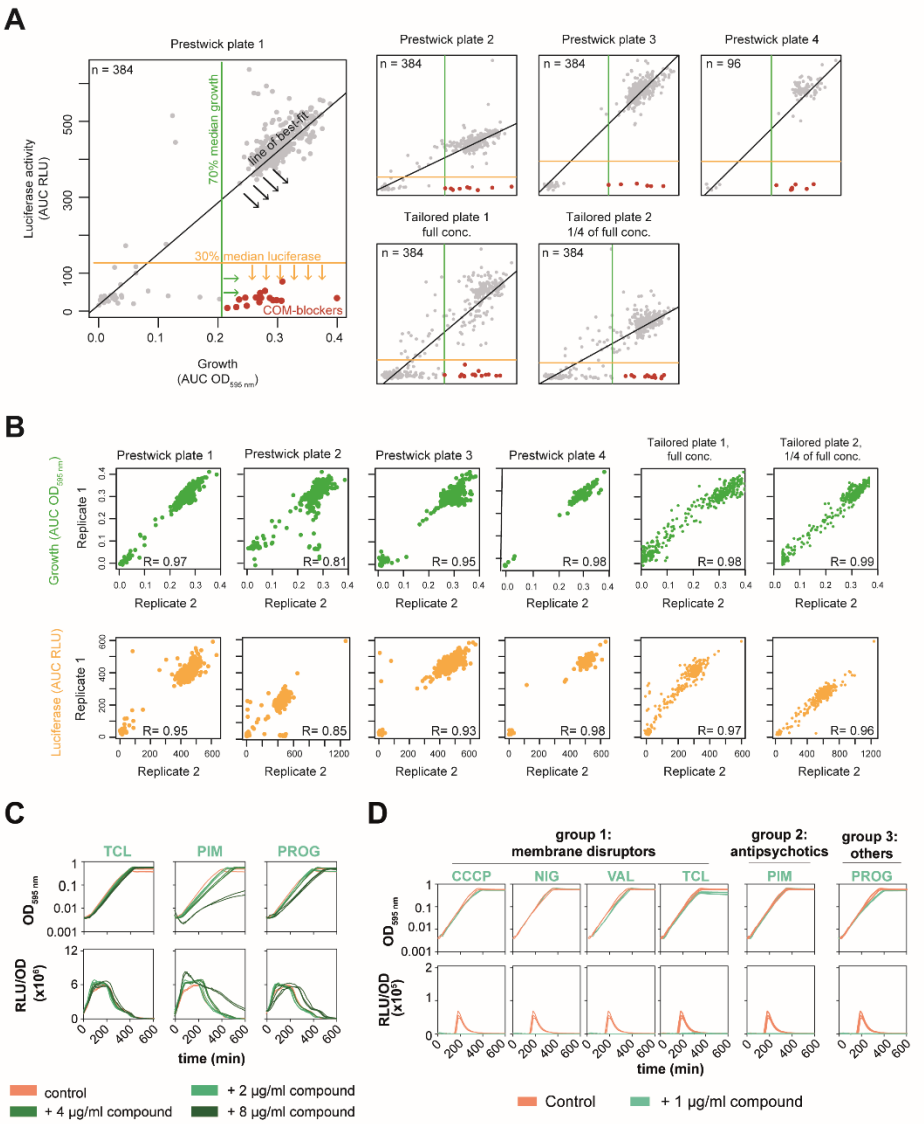

Figure S1: Identification and validation of COM-blockers from the high-throughput screen, related to Figure 1 and STAR methods**. (A)** Scatter plots show the luminescence signal (area under the curve AUC - RLU) versus growth (AUC - $OD_{595\ nm}$) obtained for each individual well per plate until 5 h of culture (Prestwick library plates 1-4, tailored library 1-2). Only one replicate per plate is shown. The green, yellow and black lines show the stringent criteria used to identify compounds that blocked natural competence development without drastically affecting growth (COM-blockers), here shown in red**. (B)** Scatter plots show the correlation between the replicates regarding their growth (green, area under the curve AUC - $OD_{595\ nm}$) as well their luminescence signal (yellow, AUC - RLU). N indicates the number of drugs (wells) per plate, and R shows that Pearson correlation coefficient. **(C)** Growth curves and constitutive expression of luciferase in presence of COM-blockers. Strain ADP9 (*cep*::P_3-*luc*) was grown in C+Y medium at pH 7.5. The addition of the compounds does not affect the luciferase production, discarding a possible interaction between both luciferin and COM-blockers. Three replicates are plotted for each condition. **(D)** Group 1 compounds that affect the membrane and/or ions homeostasis: cccp, nigericin (NIG), valinomycin (VAL) and Triclosan (TCL). The presence of 1 µg/ml of the compound does not affect the growth rates but completely blocks the bioluminescence activity and thereby competence activation. Antipsychotic pimozide (PIM; group 2) and the antimalarial proguanil hydrochloride (PROG; group 3) also block competence induction without affecting the growth rates. Three replicates are plotted for each condition.

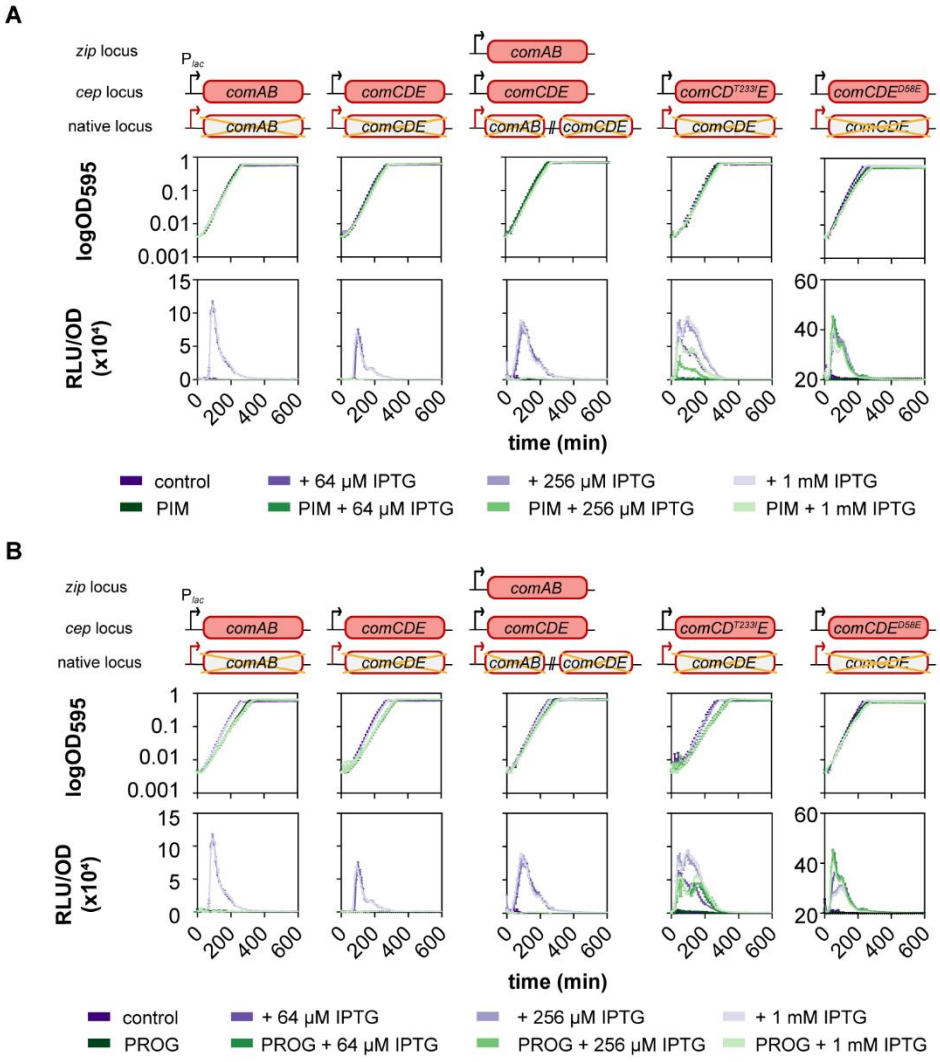

Figure S2. COM-blockers counteract the induction of *comAB* and/or *comCDE* and abolished competence, related to Figure 1D. **(A)** Pimozide (PIM) effect on growth and detection of competence development. Experiment was performed in C+Y medium at pH 7.5, permissive for natural competence. IPTG was added to the medium at the beginning at different final concentrations. Average of 3 replicates and Standard Error of the Mean (SEM) are plotted. Strains used (left to right: ADP226, ADP107, ADP350, ADP272 and ADP148). Black arrows refer to the IPTG-inducible promoter P_{lac}, while red arrows indicate native promoters. (**B**) Proguanil hydrochloride (PROG) effect on growth and detection of competence development. Identical conditions of medium and pH than in panel A. Average of 3 replicates and Standard Error of the Mean (SEM) are plotted. Strains used (left to right: ADP226, ADP107, ADP350, ADP272 and ADP148). Black arrows refer to the IPTG-inducible promoter P_{lac}, while red arrows indicate native promoters.

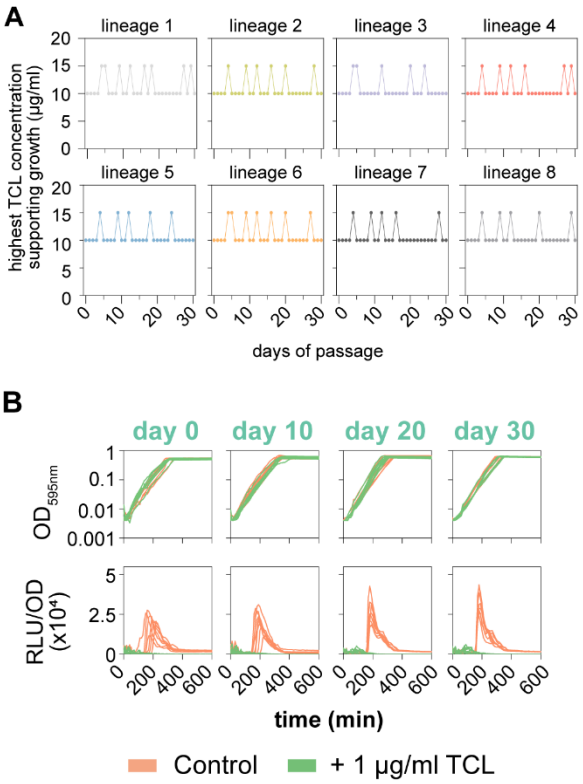

Figure S3. TCL blocks competence in several strains, with undetectable resistance development and no reduction in COM-blocking activity, related to figure 4. (**A**) Undetectable acquisition of TCL resistance after 30 days of passaging in three concentrations of TCL (10 µg/ml, 15 µg/ml and 20 µg/ml TCL). Eight independent lineages were followed (one plot per lineage). For each lineage, ten different colonies were picked. Then, bacteria were plated in freshly prepared agar plates with the indicated concentrations of TCL. Only the highest TCL concentration where cells grew are indicated. The highest concentration where we detected growth was at 15 µg/ml of TCL; however, cells were not able to grow during continuous exposure at this concentration. (**B**) Continuous exposure to TCL does not affect the ability to block competence. The pool of colonies from each individual lineage was grown in C+Y medium in permissive conditions for natural competence development (pH 7.5) in the presence or absence of 1 µg/ml of TCL.

Table S3. List of COM-blockers, related to Figure 1.

COM-blockers	Library	ATC code*
Astemizole	Prestwick	R06AX11
Bacitracin	Tailored	D06AX05, J01XX10, R02AB04
Benzalkonium	Tailored	D08AJ01
Berberine	Tailored	A07XA
CCCP	Tailored	-
Chlorhexidine	Tailored	A01AB03, D08AC02, R02AA05, D09AA12, B05CA02
Clofilium tosylate	Prestwick	C01BG
Colistin sulfate	Tailored	J01XB01, A07AA10
Estradiol Valerate	Prestwick	G03CA03
Fluoxetine hydrochloride	Prestwick	N06AB03
Fluphenazine dihydrochloride	Prestwick	N05AB02
Fluspirilen	Prestwick	N05AG01
Griseofulvin	Prestwick	D01AA08, D01BA01
Halofantrine hydrochloride	Prestwick	P01BX01
Hexachlorophene	Prestwick	D08AE01
Indatraline hydrochloride	Prestwick	-
Lidoflazine	Prestwick	C08EX01
Loperamide hydrochloride	Both	A07DA03
Meclozine dihydrochloride	Prestwick	R06AE05
Methiothepin maleate	Prestwick	N05AX
Methotrimeprazine maleat salt	Prestwick	N05AA02
Metixene hydrochloride	Prestwick	N04AA03
Niclosamide	Prestwick	P02DA01
Norgestimate	Prestwick	G03AA11, G03FA13
Penbutolol sulfate	Prestwick	C07AA23
Perphenazine	Prestwick	N05AB03
Pimozide	Prestwick	N05AG02
Pinaverium bromide	Prestwick	A03AX04
Prenylamine lactate	Prestwick	C01DX02
Prochlorperazine dimaleate	Prestwick	N05AB04
Proguanil hydrochloride	Prestwick	P01BB01
Propafenone hydrochloride	Prestwick	C01BC03
Pyrvinium pamoate	Prestwick	P02CX01
Sertraline	Prestwick	N06AB06
Spiperone	Prestwick	N05AD
Teicoplanin	Tailored	J01XA02
Terfenadine	Prestwick	R06AX12
Thiethylperazine dimalate	Prestwick	R06AD03
Thioridazine hydrochloride	Prestwick	N05AC02
Triclosan	Tailored	D08AE04, D09AA06
Trifluoperazine dihydrochloride	Prestwick	N05AB06
Triflupromazine hydrochloride	Prestwick	N05AA05
Vancomycin hydrochloride	Tailored	J01XA01, A07AA09
Verapamil hydrochloride	Tailored	C08DA01
Verteporfin	Prestwick	S01LA01
Zuclopenthixol dihydrochloride	Prestwick	N05AF02, N05AF05

*ATC: Anatomical Therapeutic Chemical Classification System.

Table S4. *In vitro* transformation assays and TCL effect, related to Figure 5.

	No. of transformants (cfu/ml)	Total viable count (cfu/ml)	Transformation efficiency
Transformation of naked DNA in the encapsulated strain D39V, planktonic growth			
D39V (negative control)	0	$5.6 \cdot 10^{11} \pm 1.3 \cdot 10^{10}$	n. a.
D39V + pLA18	$3.8 \cdot 10^{5} \pm 4.2 \cdot 10^{3}$	$5.1 \cdot 10^{11} \pm 1.6 \cdot 10^{10}$	$\mathbf{7.5 \cdot 10^{-7}} \pm 1.1 \cdot 10^{-7}$
D39V + pLA18 + 1 µg/ml of TCL	0	$5.1 \cdot 10^{11} \pm 2.6 \cdot 10^{10}$	**0**
D39V + pLA18 + 0.2 µg/ml CIP	$3.2 \cdot 10^{5} \pm 6.6 \cdot 10^{4}$	$3.4 \cdot 10^{11} \pm 5.6 \cdot 10^{10}$	$\mathbf{1.0 \cdot 10^{-5}} \pm 3.7 \cdot 10^{-7}$
D39V + pLA18 + 0.2 µg/ml CIP + 1 µg/ml TCL	0 ± 0	$3.0 \cdot 10^{11} \pm 1.4 \cdot 10^{10}$	**0**
D39V + pLA18 + 10 µg/ml GEN	$2.0 \cdot 10^{5} \pm 3.2 \cdot 10^{4}$	$5.1 \cdot 10^{11} \pm 3.3 \cdot 10^{10}$	$\mathbf{4.1 \cdot 10^{-7}} \pm 8.9 \cdot 10^{-8}$
D39V + pLA18 + 10 µg/ml GEN + 1 µg/ml TCL	0	$4.3 \cdot 10^{11} \pm 7.8 \cdot 10^{10}$	**0**
Transformation of naked DNA in an unencapsulated variant, adhered to A549 cells			
ADP25 (*Δcps*)	0	$4.1 \cdot 10^{10} \pm 2.9 \cdot 10^{9}$	n. a.
ADP25 + pLA18	$2.7 \cdot 10^{5} \pm 4.9 \cdot 10^{4}$	$4.1 \cdot 10^{10} \pm 2.2 \cdot 10^{9}$	$\mathbf{6.7} \cdot 10^{-6} \pm 2.2 \cdot 10^{-5}$
ADP25 + pLA18 + 1 µg/ml TCL	0	$3.2 \cdot 10^{10} \pm 1.9 \cdot 10^{9}$	**0**

*Average of six replicates + standard deviation. D39V was used for the planktonic experiments, while the unencapsulated variant ADP25 was used in transformation assays with human cells. Experiments were performed in C+Y medium at pH 7.5, permissive for natural competence development.

Table S5. *In vitro* HGT assays and COM-blockers effect, related to Figure 5.

	No. of transformants (cfu/ml)	Total viable count (cfu/ml)	Transformation efficiency
HGT between enapsulated strains, planktonic growth			
Horizontal gene transfer:			
DLA3 + MK134	$5.4 \cdot 10^4 \pm 6.9 \cdot 10^2$	$1.5 \cdot 10^9 \pm 2.6 \cdot 10^8$	$\mathbf{3.6 \cdot 10^{-5}} \pm 2.6 \cdot 10^{-6}$
DLA3 + MK134 + 2 µg/ml TCL	0	$1.1 \cdot 10^9 \pm 1.2 \cdot 10^8$	**0**
DLA3 + MK134 + 2 µg/ml CCCP	$1.1 \cdot 10^2 \pm 1.9 \cdot 10^2$	$7.7 \cdot 10^8 \pm 1.5 \cdot 10^8$	$\mathbf{1.4 \cdot 10^{-7}} \pm 1.3 \cdot 10^{-6}$
DLA3 + MK134 + 2 µg/ml PIM	0	$1.2 \cdot 10^9 \pm 2.5 \cdot 10^8$	**0**
DLA3 + MK134 + 2 µg/ml PROG	0	$1.1 \cdot 10^9 \pm 2.0 \cdot 10^8$	**0**
Replicative plasmid transfer:			
ADP65 + PGs6	$2.1 \cdot 10^3 \pm 1.4 \cdot 10^2$	$3.1 \cdot 10^8 \pm 2.1 \cdot 10^6$	$\mathbf{6.8 \cdot 10^{-6} \pm 4.1 \cdot 10^{-4}}$
ADP65 + PGs6 + 2µg/ml TCL	0	$2.1 \cdot 10^8 \pm 1.8 \cdot 10^6$	**0**
ADP65 + PGs6 + 4µg/ml TCL	0	$1.9 \cdot 10^8 \pm 2.0 \cdot 10^6$	**0**
HGT between unencapsulated variants, adhered to A549 cells			
ADP26 + ADP46	$1.5 \cdot 10^6 \pm 2.1 \cdot 10^5$	$3.5 \cdot 10^{10} \pm 5.0 \cdot 10^8$	$\mathbf{4.3 \cdot 10^{-5}} \pm 4.2 \cdot 10^{-4}$
ADP26 + ADP46 + 2µg/ml TCL	$1.9 \cdot 10^6 \pm 4.1 \cdot 10^5$	$2.8 \cdot 10^{10} \pm 3.2 \cdot 10^9$	$\mathbf{6.9 \cdot 10^{-5}} \pm 1.3 \cdot 10^{-4}$
ADP26 + ADP46 + 4µg/ml TCL	0	$2.1 \cdot 10^{10} \pm 7.8 \cdot 10^8$	**0**

*Average of six replicates + standard deviation. Strains DLA3 (ΔbgaA::(P_{ssbB}-*luc*, tetR), MK134 (P_{ssbB}-*ssbB_luc*, kanR), ADP73 (replicative plasmid PGs6, eryR) and ADP65 (P_{ssbB}-*ssbB_luc*, kanR + *prs1::lacI*, gmR) were used for planktonic assays. The non-capsular variants of DLA3 (ADP26) and MK134 (ADP46) were used for HGT experiments of adhered bacteria to A549 human airways cells. Experiments were performed in C+Y medium at pH 7.5, permissive for natural competence development.

Table S6. *In vivo* horizontal gene transfer (HGT) of antimicrobial determinants, related to Figure 6.

Mock			PROG		
HGT efficiency	total CFU/ml	No. of transformants	HGT efficiency	total CFU/ml	No. of transformants
5,77E-08	5,20E+08	30	6,06E-08	3,30E+08	20
1,09E-07	6,40E+08	70	2,94E-07	1,70E+08	50
1,05E-07	1,90E+08	20	1,05E-07	1,90E+08	20
6,67E-08	3,00E+08	20	3,45E-08	2,90E+08	10
8,33E-08	3,60E+08	30	0,00E+00	7,00E+07	0
7,81E-08	6,40E+08	50	8,77E-08	1,14E+08	10
9,52E-08	8,40E+08	80	0,00E+00	3,90E+08	0
3,77E-08	1,06E+09	40	1,58E-07	1,90E+08	30
6,67E-07	1,20E+08	80	1,59E-07	4,40E+08	70
2,62E-07	1,30E+09	340	0,00E+00	6,70E+08	0
3,45E-07	8,70E+07	30	1,33E-07	1,50E+08	20
1,47E-07	6,80E+07	10	0,00E+00	1,10E+08	0
8,54E-08	8,20E+08	70	2,86E-08	3,50E+08	10
5,56E-08	3,60E+08	20	0,00E+00	1,90E+08	0
7,79E-08	7,70E+08	60	2,70E-08	3,70E+08	10
1,19E-08	8,40E+08	10	3,85E-08	2,60E+08	10
5,88E-08	1,02E+09	60	0,00E+00	2,50E+08	0
3,39E-08	5,90E+08	20	0,00E+00	8,40E+07	0
1,09E-07	4,60E+08	50	0,00E+00	5,20E+08	0
4,92E-08	6,10E+08	30	2,00E-08	5,00E+08	10
3,45E-08	5,80E+08	20	0,00E+00	1,70E+08	0
1,79E-08	5,60E+08	10	1,00E-07	1,00E+08	10
3,22E-07	5,90E+08	190	0,00E+00	1,40E+08	0
0,00E+00	7,10E+08	0	0,00E+00	7,30E+08	0
			2,26E-07	3,10E+08	70
			0,00E+00	5,10E+08	0
			0,00E+00	2,60E+08	0

Strains DLA3 (Δ*bgaA*::P_{ssbB}-*luc*, *tet*^{R}) and MK134 (P_{ssbB}-*ssbB-luc*, *kan*^{R}) were used.

Table S7. MIC to representative antibiotics after continuous exposure to TCL, related to Figure 4.

Clinical antibiotic	TCL expossure	*S. pneumoniae*		
		Lineage 1	**Lineage 2**	**Mix of all 8 lineages**
Cefotaxime (µg/ml)	No TCL	0.03	0.03	0.03
	10 days	0.03	0.016 – 0.03	0.03
	20 days	0.03	0.03	0.03
	30 days	0.03	0.03	0.03
ciprofoxacin (µg/ml)	No TCL	0.5	0.5	0.5
	10 days	0.5	0.5	0.5
	20 days	0.5	0.5	0.5
	30 days	0.5	0.5	0.5
azithromycin (µg/ml)	No TCL	0.25 – 0.5	0.25	0.25
	10 days	0.25	0.25	0.25 – 0.5
	20 days	0.25 – 0.5	0.25	0.25
	30 days	0.25	0.25	0.25
tobramycin (µg/ml)	No TCL	25	25	25
	10 days	25	25	25
	20 days	25	25	25
	30 days	25	12.5	25
amikacin (µg/ml)	No TCL	50	50	50
	10 days	50	50	50
	20 days	50	50	50
	30 days	50	50	50

Table S8. Number of spontaneous colonies observed on the fluctuation assay, related to Figure 4.

Drug	24h	48h
0.03 µg/ml Rifampicin	50 (15 + 12 + 23)[a]	121 (64 + 38 + 19)
0.06 µg/ml Rifampicin	10 (2 + 3 + 5)	25 (8 + 11 + 6)
16 µg/ml TCL	0 (0 + 0 + 0)	0 (0 + 0 + 0)
32 µg/ml TCL	0 (0 + 0 + 0)	2 (1 + 0 + 1)[b]
16 µg/ml PROG	0 (0 + 0 + 0)	0 (0 + 0 + 0)
32 µg/ml PROG	0 (0 + 0 + 0)	0 (0 + 0 + 0)
16 µg/ml PIM	0 (0 + 0 + 0)	1 (0 + 0 + 1)[a]
32 µg/ml PIM	0 (0 + 0 + 0)	0 (0 + 0 + 0)

[a]The *rpoB* gene of eight random colonies was sequenced to confirm the presence of amino acid substitutions: D476L (n= 2), D476V (n= 2), V554N (n= 1), E483I (n= 1), V441N (n= 1), and no substitutions (n = 1). [b]Despite three colonies (two for TCL and one for PIM) were detected after 48h, cells were not able to grow when replated with or without the compound.

Table S9. List of strains and plasmids used in the present study, and their source, related to STAR methods.

***S. pneumoniae* strains**	**Relevant genotype**	**Reference**
D39V	Serotype 2 strain	Slager et al., 2014
DLA3	*bgaA::P$_{ssbB}$-luc*	Slager et al., 2014
MK134	*P$_{ssbB}$-ssbB-luc*	Slager et al., 2014
ADP9	*cep::P$_3$-luc*	This study
ADP25	*cps::cat*	Moreno-Gámez et al., 2017
ADP26	*bgaA::P$_{ssbB}$-luc, cps::cat*	Moreno-Gámez et al., 2017
ADP46	*ssbB-luc, cps::cat*	This study
ADP49	*PMEN14, P$_{ssbB}$-ssbB-luc*	Moreno-Gámez et al., 2017
ADP50	*PMEN18, P$_{ssbB}$-ssbB-luc*	This study
ADP65	*P$_{ssbB}$-ssbB-luc, prs1::P$_{F6}$-lacI*	This study
ADP73	*pPGs6*	This study
ADP85	*bgaA::P$_{ssbB}$-luc, prs1::P$_{F6}$-lacI, cep::P$_{lac}$-comE*	This study
ADP95	*bgaA::P$_{ssbB}$-luc, prs1::P$_{F6}$-lacI*	Moreno-Gámez et al., 2017
ADP107	*bgaA::P$_{ssbB}$-luc, prs1::P$_{F6}$-lacI, cep::P$_{lac}$-comCDE, comCDE::cat*	Moreno-Gámez et al., 2017
ADP110	*bgaA::P$_{ssbB}$-luc, prs1::P$_{F6}$-lacI, cep::P$_{lac}$-comE, comE::cat*	This study
ADP129	*comCDE-luc*	This study
ADP137	*comAB-luc*	This study
ADP138	*bgaA::P$_{ssbB}$-luc, prs1::P$_{F6}$-lacI, cep::P$_{lac}$-comD*	This study
ADP140	*bgaA::P$_{ssbB}$-luc, prs1::P$_{F6}$-lacI, cep::P$_{lac}$-comD, comD*stop*	This study
ADP145	*bgaA::P$_{ssbB}$-luc, prs1::P$_{F6}$-lacI, cep::P$_{lac}$-comCDE^{D58E}*	This study
ADP148	*bgaA::P$_{ssbB}$-luc, prs1::P$_{F6}$-lacI, cep::P$_{lac}$-comCDE^{D58E}, comCDE::cat*	This study
ADP166	*bgaA::P$_{lac}$-dCas9sp, prs1::P$_{F6}$-lacI, cep::P$_3$-sgRNA-atpC, P$_{ssbB}$-ssbB-luc*	This study
ADP168	*bgaA::P$_{lac}$-dCas9sp, prs1::P$_{F6}$-lacI, cep::P$_3$-sgRNA-atpA, P$_{ssbB}$-ssbB-luc*	This study
ADP172	*bgaA::P$_{lac}$-dCas9sp, prs1::P$_{F6}$-lacI, cep::P$_3$-sgRNA-atpE, P$_{ssbB}$-ssbB-luc*	This study
ADP226	*bgaA::P$_{ssbB}$-luc-gfp, prs1::P$_{F6}$-lacI, cep::P$_{lac}$-comAB, comAB::ery*	Moreno-Gámez et al., 2017
ADP265	*bgaA::P$_{lac}$-dCas9sp, prs1::P$_{F6}$-lacI, cep::P$_3$-sgRNA-atpC, cil::P$_3$-luc*	This study
ADP268	*bgaA::P$_{lac}$-dCas9sp, prs1::P$_{F6}$-lacI, cep::P$_3$-sgRNA-atpA, cil::P$_3$-luc*	This study
ADP270	*bgaA::P$_{lac}$-dCas9sp, prs1::P$_{F6}$-lacI, cep::P$_3$-sgRNA-atpE, cil::P$_3$-luc*	This study
ADP271	*bgaA::P$_{ssbB}$-luc, prs1::P$_{F6}$-lacI, cep::P$_{lac}$-comCD^{T233I}E*	This study
ADP272	*bgaA::P$_{ssbB}$-luc, prs1::P$_{F6}$-lacI, cep::P$_{lac}$-comCD^{T233I}E, comCDE::cat*	This study
ADP279	*bgaA::P$_{ssbB}$-luc*, atpE^{V48L}	This study
ADP280	*bgaA::P$_{ssbB}$-luc*, atpE^{A49T}	This study
ADP308	*zip::P$_{comC}$-comC'_HiBiT*	Domenech et al., 2018
ADP311	*zip::P$_{comC}$-comC'_HiBiT + comAB::ery*	Domenech et al., 2018
ADP312	*zip::P$_{comC}$-HiBiT*	Domenech et al., 2018
ADP326	*zip::P$_{lac}$-HiBiT*	This study
ADP342	*bgaA::P$_{ssbB}$-luc, comAB::ery*	This study
ADP349	*bgaA::*P$_{ssbB}$*-luc, prs1::*P$_{F6}$*-lacI-tetR, cep::*P$_{lac}$*-comAB, comAB::ery, zip::*P$_{lac}$*-comCDE*	This study

ADP350	*bgaA*::P_{ssbB}-*luc, prs1*::P_{F6}-*lacI-tetR, cep*::P_{lac}-*comAB, comAB::ery, zip*::P_{lac}-*comCDE, comCDE::cat*	This study
PMEN1	Spain^{23F}-1	GNRCS[b]
PMEN3	Spain^{9V}-3	GNRCS[b]
ST6521	Spain^{9V}-3 expressing capsular type 11A	GNRCS[b]
PMEN14	Taiwan^{19F}-14	Radboud[a]
PMEN18	Tennessee^{14}-18	Radboud[a]
PMEN19	Colombia^{5}-19	GNRCS[b]
PMEN25	Sweden^{15A}-25	GNRCS[b]
PMEN28	Sweden^{1}-28	GNRCS[b]
PMEN31	Netherlands^{3}-31	GNRCS[b]
TIGR4	Serotype 4 strain	GNRCS[b]
Other bacteria		
ADP51	*S. mitis* NTCC10712, *ssbB-luc*	Moreno-Gámez et al., 2017
ADP53	*S. sanguis* V683, *ssbB-luc*	This study
PA14	*Pseudomonas aeruginosa*	-
Plasmids		
pLA18	Integrates in *bgaA::*P_{ssbB}*-luc-gfp*	Slager et al., 2014
pPEP23	Integrates in *cep::*P_3*-luc*	Slager et al., 2014
pPGs6	Non-integrative plasmid	Yuzenkova et al., 2014

[a]Strains provided by Prof. P. Hermans, from Laboratory of Pediatric Infectious Diseases, Department of Pediatrics, Radboud University Medical Center, Nijmegen, The Netherlands. [b]Strains provided by PhD. MPG Van der Linden, from Germany National Reference Center for Streptococci, Institute of Medical Microbiology, University Hospital RWTH Aachen, Aachen, Germany. Abbreviations: LB ans SB referrer to the Large Bit and Small Bit of the Nanoluc enzyme, respectively. **Strains contruction**: **ADP9:** the plasmid pPEP23 (Slager et al., 2014), containing the P_3-*luc* construct was transformed into *S. pneumoniae* D39V (P_3 promotor drives the constitutive expression of luciferase). **ADP46:** the PCR product of the capsular operon deletion, replaced by the chloramphenicol resistance cassette (*cps::cat*), was amplified from ADP25 strain transformed into the MK134 strain (Slager et al., 2014). **ADP50 and ADP53:** the PCR fragment P_{ssbB}-*ssbB-luc* including the kanamycin resistance cassette (MK134 strain), was transformed into the pneumococcal international clone PMEN18, and the reference strain *Streptococcus sanguinis* V683. **ADP65:** the PCR fragment *prs1::*P_{F6}-*lacI* including the gentamycin resistance cassette (Liu et al., 2017), was transformed into the MK134 strain. **ADP73:** the replicative plasmid pPGs6 (Yuzenkova et al., 2014) was transformed to D39V strain. **ADP148:** using the ADP107 strain as a template (*cep*::P_{lac}-*comCDE*), a point mutation in comE gene (T174G) was introduced by overlapping PCR, using primers ADP3/65 (CATGAATATCGATCTCTAGGAAATAAAGC) and ADP3/66 (GCTTTATTTCCTAGAGATCGATATTCATG). This point mutation results in an amino acid replacement (ComE^{D58E}). The product was transformed into ADP95, resulting in strain ADP145. Then, the PCR product of Δ*comCDE::cat* from ADP107 strain was transformed into ADP145, resulting in strain ADP148. **ADP272:** using the strain ADP107 as template (*cep*::P_{lac}-*comCDE*), a point mutation in comD gene (C1719T) was introduced by overlapping PCR, using primers ADP2/19 (GACCAACAATTTCATCTATGTAATTCTGT) and ADP2/20 (ACAGAATTACATAGATGAAATTGTTGGTC). The product was transformed into ADP95, resulting in strain ADP271. Then, the PCR product of Δ*comCDE::cat* from ADP107 strain was transformed into ADP271, resulting in strain ADP272. **ADP166, ADP168 and ADP172:** to confirm whether pH homeostasis is essential for competence, we used three CRISPRi strains, with sgRNAs targeting three genes of the operon encoding the ATP synthase: *atpC*, *atpA* and *atpE* (strains #342, #349 and #362, respectively (Liu et al., 2017) . P_{ssbB}-*ssbB-luc* fragment including the kanamycin resistance cassette (MK134 strain) was transformed into these three strains. **ADP265, ADP268 and ADP270:** the PCR fragment P_3-*luc* with integration into the intergenic sequence between gene loci *spd_0422* and *spd_0423* was transformed into the above mentioned strains #342, #349 and #362. **ADP110:** we constructed a suite of strains in which we could ectopically induce competence genes by the addition of IPTG, with the deletion of the original locus. To amplify *comD*, primers ADP4/37 (CAGTAGATCTAGGAGGAGAGTAATGGATTTATTTGGATTTG) and ADP2/65 (ACGTCTCGAGACTAGTCATTCAAATTCCCTCTTAAATC) were used. To amplify *comE*, primers ADP2/76 (ACTGAGATCTGACAAATCATTAGATTTAAGAGGG) and ADP2/58 (ACGTCTCGAGGCGGCCGCCAATTTCTTGCTAATTGTC) were used, with D39V strain as a template for both fragments. PCR products were digested with BglII and XhoI and were ligated with similarly digested pPEP1 plasmid

containing the P_{lac} promoter (Liu et al., 2017). The ligations were transformed into strain ADP95, resulting in strains ADP138 and ADP85, respectively. To these strains, either the PCR product *ΔcomD** (clean mutant) or *ΔcomE::cat* was transformed into those strains, resulting in strains ADP110 and ADP140. **ADP129 and ADP137:** the firefly luciferase *luc* was fused to *comAB* and *comCDE* operons. For ADP129 strain, we PCR-ed the *comCDE-luc* fragment including the kanamycin resistance marker, from strain DJS29 (Slager et al., 2014). For the *comAB-luc* construct, the upstream region of *comAB* was amplified using primers ADP2/75 (AGGAGAGGATGAAACCAGAATTTTTAG) and ADP2/56+XhoI (ACTGACTAGTCTCGAGCACGAACATTACTCTTTGTTCAA), the downstream region with primers ADP3/33+NotI (CAGTGCGGCCGCTATTTATTCGGTTAAATTCTTGTG) and ADP2/45 (CAGCCTTTTTTTCAACAAAAATACGTTTATC), and the luc gene including the kanamycin resistance marker (from MK134 strain) with ADP4/36+XhoI (CAGTCTCGAGGCTGAAGGAGGAATAATGAGATCCG) and PG97+NotI (CAGTGCGGCCGCTCTAGGTACTAAAACAATTC). All three fragments were digested with the proper restriction enzymes (NotI and/or XhoI) and ligated. **ADP279 and ADP280**: To test whether two different point mutations in *atpE* ($AtpE^{V48L}$ and $AtpE^{A49T}$) could cause a loss of susceptibility and/or activity of COM-blockers, we introduced the SNP by overlapping PCR using primers OVL1385 (TGTTTTTAGGTGTTACCTTTATTGAAGGAAC) and OVL1386 (GTTCCTTCAATAAAGGTAACACCTAAAAACA) for $atpE^{A49T}$, and primers OVL1387 (TGTTTTTAGGTCTTGCCTTTATTGAAGGAAC) and OVL1388 (GTTCCTTCAATAAAGGCAAGACCTAAAAACA) for $atpE^{V48L}$, Both fragments were transformed into DLA3, resulting in strains ADP279 and ADP280, respectively. **ADP326:** we overlapped the ADP325 construct with primers OVL2328 (CACCACCACCCATAATAAAATCTCCTTATTTATTTAGATCTTAATTGTGAG) and OVL2329 (CTCACAATTAAGATCTAAATAAATAAGGAGATTTTATTATGGGTGGTGGTG) to remove the leader peptide sequence. Overlapped fragment was transformed into D39V strain. **ADP350:** primers ADP2/38 (CAGTGGATCCGGTTTTTGTAAGTTAGCTTACAAG) and ADP2/58 (ACGTCTCGAGGCGGCCGCCAATTTCTTGCTAATTGTC) were used to amply *comCDE*, with D39V strain as a template. PCR product was digested with BamHI and XhoI and were ligated with similarly digested pPEPZ plasmid containing the P_{lac} promoter (Liu et al., 2017). The ligation was transformed into strain ADP226 resulting in strain ADP349. Then, *comCDE::cat* fragment from strain ADP107 was transformed into ADP349 resulting in strain ADP350. All transformants were selected on Columbia blood agar containing the appropaite antibiotic and correct colonies were verified by PCR and sequencing.